

# **GRAND CHALLENGES IN SPACE TECHNOLOGY: DISTRIBUTED SATELLITE SYSTEMS**

**David W. Miller, Raymond J. Sedwick**

**MIT Space Systems Laboratory  
77 Mass Ave. Rm 37-371  
Cambridge, MA 02139**

**July 2001**

**Final Report**

20030624 015

**APPROVED FOR PUBLIC RELEASE; DISTRIBUTION IS UNLIMITED.**



**AIR FORCE RESEARCH LABORATORY  
Space Vehicles Directorate  
3550 Aberdeen Ave SE  
AIR FORCE MATERIEL COMMAND  
KIRTLAND AIR FORCE BASE, NM 87117-5776**

---

AFRL-VS-TR-2001-1090

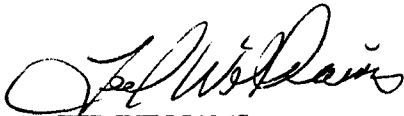
Using Government drawings, specifications, or other data included in this document for any purpose other than Government procurement does not in any way obligate the U.S. Government. The fact that the Government formulated or supplied the drawings, specifications, or other data, does not license the holder or any other person or corporation; or convey any rights or permission to manufacture, use, or sell any patented invention that may relate to them.

This report has been reviewed by the Public Affairs Office and is releasable to the National Technical Information Service (NTIS). At NTIS, it will be available to the general public, including foreign nationals.

If you change your address, wish to be removed from this mailing list, or your organization no longer employs the addressee, please notify AFRL/VSSV, 3550 Aberdeen Ave SE, Kirtland AFB, NM 87117-5776.

Do not return copies of this report unless contractual obligations or notice on a specific document requires its return.

This report has been approved for publication.



TED WILLIAMS  
Project Manager

FOR THE COMMANDER



KIRT S. MOSER, DR-IV  
Chief, Spacecraft Technology Division

<b>REPORT DOCUMENTATION PAGE</b>			<i>Form Approved</i> <b>OMB No. 0704-0188</b>	
Public reporting burden for this collection of information is estimated to average 1 hour per response, including the time for reviewing instructions, searching existing data sources, gathering and maintaining the data needed, and completing and reviewing this collection of information. Send comments regarding this burden estimate or any other aspect of this collection of information, including suggestions for reducing this burden to Department of Defense, Washington Headquarters Services, Directorate for Information Operations and Reports (0704-0188), 1215 Jefferson Davis Highway, Suite 1204, Arlington, VA 22202-4302. Respondents should be aware that notwithstanding any other provision of law, no person shall be subject to any penalty for failing to comply with a collection of information if it does not display a currently valid OMB control number. <b>PLEASE DO NOT RETURN YOUR FORM TO THE ABOVE ADDRESS.</b>				
<b>1. REPORT DATE (DD-MM-YYYY)</b> 01-07-2001		<b>2. REPORT TYPE</b> Final Report		<b>3. DATES COVERED (From - To)</b> 01/06/1997 to 01/04/2001
<b>4. TITLE AND SUBTITLE</b> Grand Challenges in Space Technology: Distributed Satellite Systems		<b>5a. CONTRACT NUMBER</b> F29601-97-K-0010		
		<b>5b. GRANT NUMBER</b>		
		<b>5c. PROGRAM ELEMENT NUMBER</b> 63285E		
<b>6. AUTHOR(S)</b> David W. Miller, Raymond J. Sedwick		<b>5d. PROJECT NUMBER</b> DARP		
		<b>5e. TASK NUMBER</b> SV		
		<b>5f. WORK UNIT NUMBER</b> BD		
<b>7. PERFORMING ORGANIZATION NAME(S) AND ADDRESS(ES)</b> MIT Space Systems Laboratory 77 Mass Ave. Rm 37-371 Cambridge, MA 02139		<b>8. PERFORMING ORGANIZATION REPORT NUMBER</b>		
<b>9. SPONSORING / MONITORING AGENCY NAME(S) AND ADDRESS(ES)</b> Air Force Research Laboratory Space Vehicles Directorate 3550 Aberdeen Ave., SE Kirtland AFB, NM 87117-5776		<b>10. SPONSOR/MONITOR'S ACRONYM(S)</b>		
		<b>11. SPONSOR/MONITOR'S REPORT NUMBER(S)</b> AFRL-VS-TR-2001-1090		
<b>12. DISTRIBUTION / AVAILABILITY STATEMENT</b> APPROVED FOR PUBLIC RELEASE; DISTRIBUTION IS UNLIMITED.				
<b>13. SUPPLEMENTARY NOTES</b>				
<b>14. ABSTRACT</b>  The MIT/AFRL Distributed Satellite Systems program examines the motivation, analysis and development of technology associated with the distribution of assets and functionality over a number of cooperating satellites. A complete framework (GINA) for the analysis and comparison of widely varying architectures has been developed and applied to various test cases both existing and in development. Many technologies have been studied, including space based interferometric radar and imaging, formation flying dynamics and control of clusters, micropropulsion, launch vehicle selection, software development and mechanisms for end of life disposal. Two test beds have been developed for the purpose of validating the theories and exercising autonomy and control. This paper summarizes the findings of this research.				
<b>15. SUBJECT TERMS</b> distributed satellite systems, GINA, interferometric radar, orbital dynamics, micropropulsion system selection, satellite clusters, spheres, satellite formation flight				
<b>16. SECURITY CLASSIFICATION OF:</b>			<b>17. LIMITATION OF ABSTRACT</b>  SAR	<b>18. NUMBER OF PAGES</b>  84
<b>a. REPORT</b> Unclassified	<b>b. ABSTRACT</b> Unclassified	<b>c. THIS PAGE</b> Unclassified		
			<b>19b. TELEPHONE NUMBER (include area code)</b> (505) 853-3428	



## TABLE OF CONTENTS

1.1	Advantages of Distribution .....	1
1.2	To Distribute or Not to Distribute.....	6
1.3	Developed Tools and Technologies.....	6
2.0	TECHNICAL RESEARCH AREAS .....	9
2.1	Generalized Information Network Analysis (GINA).....	9
2.2	Scanned Pattern Interferometric Radar .....	12
2.3	Separated Spacecraft Imagers .....	16
2.4	Orbital Dynamics for Separated Spacecraft Clusters.....	21
2.5	Formation Flight Maneuver Optimization .....	25
2.6	Micropropulsion System Selection for Precision Formation Flying Satellites .....	30
2.7	Software Architecture for Satellite Formation Flight.....	34
2.8	Evolutionary Growth of Mission Capability .....	39
2.9	Optimization Approach to the Launch Vehicle Selection Process for Satellite Constellations .....	43
2.10	A Systems Study on How to Dispose of Fleets of Small Satellites.....	47
2.11	Performance Analysis of a Space-Based GMTI Radar System .....	50
2.12	SPHERES: A Testbed for Long Duration Satellite Formation Flight.....	53
2.13	Acoustic Imaging Testbed for Spacecraft Cluster Autonomy.....	58
2.14	Generalized Flight Operations Processing Simulator .....	61
3.0	CONCLUSIONS.....	66
	References .....	69
	Bibliography .....	70
	Bibliography of DSS Publications (Referenced by CD Section).....	73

## FIGURES

Figure 1. TPF Global Trade Space and Zoom-In of the Most Cost-Effective Region.....	11
Figure 2. An Example of the SPIR Methodology.....	14
Figure 3. Point Spread Function Matrix for an 8-Satellite Unrestricted Array.....	15
Figure 4. Recovered Signal for a Footprint Strip with Two Targets.....	16
Figure 5. Variation of $\Delta V/n^2 R_o T_{life}$ as array's LOS is varied.....	18
Figure 6. Exploitation of conic section properties in the second DSS architecture.....	18
Figure 7. Delay line length required for imaging terrestrial targets.....	19
Figure 8. Total architecture mass as a function of number of collector spacecraft.....	21
Figure 9. Radial Error (m) of Estimated Position Over Time.....	24
Figure 10. In-Track Error (m) of Estimated Position Over Time.....	24
Figure 11. Cross-Track Error (m) of Estimated Position Over Time.....	24
Figure 12. Average energy required per spacecraft.....	27
Figure 13. Maximum power required to initialize a cluster of $N$ spacecraft.....	28
Figure 14. Average $\Delta V$ required per spacecraft to initialize a cluster of $N$ spacecraft.....	28
Figure 15. Maximum power required to re-size the Techsat 21 cluster.....	29
Figure 16. Average $\Delta V$ required to re-size a cluster of 3 spacecraft.....	29
Figure 17. SPECS propulsion system total costs including.....	33
Figure 18. Software Architecture Effects on Communication Requirements.....	37
Figure 19. Formation Flight Experimental Results – 90° Slew Maneuver.....	38
Figure 20. Concept for deploying aperture in a staged manner.....	40
Figure 21. Fill factor and cost ratio versus number of spacecraft.....	41
Figure 22. Total Launch Costs For Different Objective Functions in the Three Case Studies.....	46
Figure 23. Most efficient disposal options for average density spacecraft.....	48
Figure 24. Most efficient disposal options for silicon satellites.....	50
Figure 25. Top Level View of the TechSat 21 GINA Model.....	51
Figure 26. Aerospace Corporation Baseline Design Trade Space (a) and Trade Space Zoom-In (b).....	52
Figure 27. Multi-Dimensional Trade Space for TechSat21.....	52
Figure 28. SPHERES Testbed Overview.....	54
Figure 29. The SPHERES Propulsion Subsystem.....	54
Figure 30. Software Architecture.....	56
Figure 31. The SPHERES Metrology System.....	56
Figure 32. Master/Slave: Master Fixed to KC-135 Frame.....	57
Figure 33. a) Interferometer Geometry      b) 40 Baseline Sampling Pattern.....	59
Figure 34. a) 40 Baseline, Ideal Response      b) 40 Baseline, Meas. Response.....	60
Figure 35. a) 40 Baseline, 2 Sources      b) Processed 40 Baseline Image (1 source).....	61
Figure 36. Schematic of GFLOPS Testbed Hardware.....	63

## TABLES

Table 1. Results using Cornwell Configurations for Broad Band Imaging .....	19
Table 2. Architecture mass contributing elements.....	20
Table 3. SPECS Propulsion System Designs Summary .....	32
Table 4. Propulsion System Cost-Based Selection Summary.....	34
Table 5. Summary of Formation Flight Architectures Requirements.....	38
Table 6. Total Error (area between the curves) of Formation Flight Slew .....	39
Table 7. Integer Programming Formulation of the Launch Vehicle Selection Problem..	45
Table 8. Characteristics of the Three Satellite Constellation Case Studies .....	46
Table 9. Micro-Processors of each SPHERES Unit.....	55
Table 10. GFLOPS Hardware List.....	64





## **1.0 Summary: Distributed Satellite Systems**

The development of small, low cost satellites offers new horizons for space applications when several satellites operate cooperatively. The vision of what can be achieved from space is no longer bound by what an individual satellite can accomplish. Rather, the functionality can be spread over a number of cooperating satellites. Further, the modular nature of these distributed systems allow the possibility of selective upgrading as new capabilities become available in satellite technology. Similar to how business has embraced networked desktop computing over mainframes, Distributed Satellite Systems (DSS) open up the opportunity to achieve new capabilities while using relatively inexpensive, perhaps disposable components.

In the next ten to twenty years, the world will see the development of a variety of distributed satellite systems. A constellation of satellite clusters can provide space-based radar with ground resolutions much finer than current capabilities. Low Earth orbit constellations can provide telephony and data services to remote locations as well as worldwide. Formation flown telescopes can achieve angular resolutions unimaginable with monolithic telescope technology thereby enabling exo-solar planet detection and characterization.

Applications of DSS do not stop there. Political pressures in the military arena to move American troops out of harms way, yet project global superiority, has caused the Air Force to rely more heavily on cost-effective space assets. NASA's mantra of "faster, better, cheaper" has also forced cost to be a design variable. As a result, new systems engineering practices are needed which marry lifecycle cost with customer value metrics of productivity, quality of service, and design sensitivity in order to provide the customer (which includes the investors) with quantitative analysis in the early mission design stages. The INCOSE Systems Engineering Handbook states that "the need for a well-integrated approach to system design and development can be better appreciated when it is realized that approximately eighty to ninety percent of the development cost of a large system is predetermined by the time only five to ten percent of the development effort has been completed."

To this end, the Air Force Research Laboratory initiated a program in 1997 with the MIT Space Systems Laboratory to develop a quantitative methodology for synthesis and comparative analysis of DSS mission architectures as well as some of their key technological enablers. This report provides an overview of the program's objectives, motivation, results, and future direction.

### **1.1 Advantages of Distribution**

The advantages of distribution are numerous, as are the potential disadvantages. Therefore, when trading the cost-benefit of different levels of distribution within a mission, it is necessary to carefully model its impact. The following are benefits of distribution identified by MIT accompanied by a brief description of the benefit.

### **1.1.1 Decentralization of Resources**

The "resources" of a satellite system are the payloads that provide the desired information to the customer, whether that information be scientific data for a civilian agency, imagery for a defense agency, multimedia for a commercial organization, or navigation data for any of the above three entities. Decentralization refers to the fact that in a Distributed Satellite System, these payloads are dispersed among several spacecraft. For example, a suite of Earth observation instruments that would conventionally fly on a single polar orbiting weather satellite in LEO might be distributed between three separate, smaller satellite buses in the same orbital plane. In the original configuration, a failure of the spacecraft bus, such as might occur due to the malfunction of the attitude control computer, would render the entire suite of instruments (ie. *all* of the resources) useless. In the DSS configuration, only the payloads on the bus that fails are lost, while the instruments on the two remaining spacecraft may still be used. Thus, the decentralization of resources may improve the *availability* of a system. Likewise, decentralization of assets in a military space system can improve the *survivability* of the system in times of conflict.

### **1.1.2 Smaller, Simpler Satellites**

By distributing resources on multiple satellite platforms rather than placing all instruments on a single platform, smaller satellite buses may be used. This in turn results in a direct *savings in the manufacturing cost* of each satellite. Additionally, the production of smaller, simpler satellite buses is faster than for larger satellite buses. Thus, the use of distributed architectures can also *reduce the time to the Initial Operating Capability (IOC)* of a space system.

### **1.1.3 Mass Production of Satellites**

By employing the use of multiple identical satellite platforms, Distributed Satellite Systems motivate the "mass production" of satellites. The resulting economies of scale promote *learning curve savings*, reducing the cost of each satellite. Additionally, mass production of identical units also simplifies the integration and testing process, *reducing the time to IOC* and potentially *improving the reliability* of the system.

### **1.1.4 Modular Designs**

Distributed Satellite Systems promote modular designs. A modular satellite bus design is one which provides the capability to support different payloads. Different components of the bus may be incrementally upgraded or downgraded depending upon the characteristics of the given payload. Take the example of the three weather satellites orbiting in the same plane. One satellite may require larger solar arrays and more batteries because its payload suite requires more power than the payload suites on the other two satellites, while another satellite might suffice with smaller reaction wheels because its payload is less massive. While such particular characteristics may vary between satellites, the core bus design remains the same in a modular design. Modular designs promote mass production of satellite buses, leading to the same *reductions in cost and time to IOC* as previously explained. Modular designs also allow for easy *upgradability*, as newer, more advanced payload and bus technologies may be integrated with the same modular bus by employing standardized interfaces.

### **1.1.5 Spatial Distribution**

Spatial distribution involves the use of multiple satellites in different orbits. Using more satellites in a distributed system *reduces the revisit time* to a particular target on the Earth. Spatial distribution can also improve the *isolation*, *rate*, and *integrity* capabilities of a space system.

### **1.1.6 Reduced Range to Target**

In certain cases, utilization of a distributed architecture can reduce the required range to target. Take the example of a space based radar (SBR) system designed to identify and track military targets in theaters of conflict. A conventional design employs a few satellites in MEO or GEO to cover the globe. Since each satellite must be capable of satisfying the radar mission individually over its field of view, large antennas and amounts of power are required to execute the mission. This results in the use of large, expensive satellites. A distributed architecture employs the use of symbiotic clusters to fulfill the same mission. Since each target is now illuminated by multiple spacecraft rather than a single spacecraft, smaller antennas and lower Earth orbits may be used. This in turn *reduces the total power-aperture* required of each satellite, which in turn *reduces the total cost* of the system. Reducing the range to target also improves the *isolation capability* of a system (higher resolution or optical payloads) and the *integrity* of the information being transmitted throughout the network.

### **1.1.7 Separated, Sparse Apertures**

Distributed Satellite Systems promote the use of separated, sparse apertures for surveillance missions. While the angular resolution of a conventional single aperture telescope is proportional to the diameter of the primary mirror of that telescope, the angular resolution of a sparse aperture is proportional to the maximum baseline between two elements (mirrors) of the sparse aperture. Thus, Distributed Satellite Systems enable greater angular resolutions than possible with single satellite designs, improving the *isolation* capability of the system.

### **1.1.8 Multiple Viewing Angles**

Spatially distributing resources over many satellites in a Distributed Satellite System also increases the number of viewing angles between the system and the target. For example, increasing the number of satellites in a telephony constellation decreases the probability that the user telephone on the ground will not be able to communicate with a satellite in the constellation via a direct link due to line-of-sight obstruction by buildings and other tall objects. Similarly, the more satellites there exist in a global navigation system, the more likely the GPS receiver on the ground will be able to identify four satellites with good viewing angles to enable an accurate positioning measurement. Thus, the multiple viewing angles promoted by Distributed Satellite Systems improve the *availability* and *rate* of space-based systems.

### **1.1.9 Reduced Computational Workload**

Distributed Satellite Systems distribute the resources of a space system across many platforms. One these resources are space-qualified computers. Due to time consuming radiation-hardening

and other qualification procedures, the capability (speed and memory) of space-qualified computers is always several generations behind their ground-based counterparts. Certain missions however, such as the space-based radar (SBR) mission, require a tremendous amount of computational power to process the signal data and identify targets in real time. No space-qualified computer is capable of executing such computations in real time, making it unlikely that a single SBR satellite could safely cover the theater of interest. A DSS approach to the SBR mission divides the computations among the many computers on different platforms. By processing different portions of the same signal information in parallel, such a complicated mission might just become feasible with a Distributed Satellite System. Reducing the computational workload in this manner reduces computational *costs* while increasing the system *rate*.

#### **1.1.10 More Satellites**

Distributed Satellite Systems promote the use of many smaller satellites over a few larger satellites. Having more total satellites in a space system improves *survivability*, *revisit times*, and *coverage geometry*. If properly designed, more satellites can also improve the total capability of the system in terms of *isolation*, *rate*, *integrity*, and *availability*.

#### **1.1.11 Task Division**

In a collaborative DSS architecture, the responsibilities of each satellite decrease linearly with the number of satellites in the system. Each satellite can allocate more of its resources to each source, satisfying *higher rate* requirements. Increasing the number of satellites in the cluster yields linear increases in the achievable rate of information flow from each source. The limit is reached when each satellite is dedicated to a single user. The maximum rate for that user is the maximum supportable rate of the satellite.

#### **1.1.12 Increased Signal-to-Noise (SNR)**

In a symbiotic DSS architecture, the SNR of an active or passive surveillance system increases proportionally to the number of satellite in the system. Higher SNRs in turn boost the *integrity* and *rate* of the system.

#### **1.1.13 Clutter Rejection**

Symbiotic Distributed Satellite Systems can help to reduce the clutter in certain applications. Once again, take the example of an SBR system. As a direct result of the smaller beamwidths that are characteristic of symbiotic systems, the clutter rejection of the system is greatly improved compared to single satellites or collaborative systems. This in turn improves the measured SNR and increases the *integrity* and *rate* of the system.

#### **1.1.14 Redundancy**

Distributed Satellite Systems provide an inherent redundancy in space systems. Failure of a single satellite within a cluster or constellation does not prevent the system from accomplishing its mission, but may decrease the system capability. This holds true for all of the example

missions previously discussed – weather surveillance, SBR, and telephony. Thus, the redundancy provided by Distributed Satellite Systems improves the *reliability* and *availability* of space assets.

#### **1.1.15 Path Diversity**

The benefits of path diversity in Distributed Satellite Systems parallel those provided by redundancy. According to the Generalized Information Network Analysis (GINA) theory, any satellite system may be transformed into an information network where each satellite or satellite payload is a node in the network. Distributed Satellite Systems provide more nodes in the network through which information may flow than conventional single satellite deployments. In the case of a satellite failure, there are more alternative routes in the DSS for the information to arrive to the final user. In this manner, path diversity also improves the *reliability* and *availability* of a space system.

#### **1.1.16 Deployment**

Systems engineers struggle with the need to package a satellite within the geometric constraints of a launch vehicle and then deploy elements to form a larger shape while meeting the geometric accuracy needed to perform the mission. Distributed satellites allow system elements to be packaged in configurations that are more favorable for launch. This can include packaging in multiple launch vehicles. Once on orbit, the elements can be flown in formation and interconnected via soft interfaces such as relative navigation, control, and communication. Furthermore, the elements could actually be docked and aligned to form monolithic systems.

#### **1.1.17 Staged Deployment**

Collaborative distributed systems offer the possibility of being able to ramp up the investment gradually to match the development of the market. Only those satellites needed to satisfy the early market are initially deployed. If and when additional demand develops, the constellation can be augmented. The cost of constructing and launching these additional satellites is incurred later in the system lifetime. Due to the time value of money, the delayed expenditure can result in significant *cost* savings.

#### **1.1.18 Minimization of Failure Compensation**

The decentralization of resources, inherent redundancy, and path diversity in Distributed Satellite Systems minimize failure compensation costs. Recall the polar orbiting weather satellite system in LEO previously discussed under the decentralization of resources heading. If a single primary (mission critical) instrument fails in the conventional design with the entire suite of instruments on a single satellite in each plane, a new satellite with the entire suite of new instruments must be immediately launched on a large launch vehicle. Thus, all of the instruments are launched as replacements, even though all but one of the instruments are working properly. This is inherently expensive. If a primary instrument fails in the distributed architecture with the full suite of instruments divided between three satellites in each plane, then only the instruments on the failed satellite need be launched on a smaller spacecraft bus and launch vehicle. Over a long

mission, the lower failure compensation (replacement) costs can reduce the total lifecycle *cost* in a distributed satellite system.

### **1.1.19 Multi-Mission Capability**

Distributed Satellite Systems are more amenable to fulfilling multi-mission roles than single satellite deployments. This capability results from the flexibility provided by having multiple reconfigurable spacecraft. For example, a DSS design for a spaced-based radar system primarily intended for a ground-moving-target-indication (GMTI) mission may also be tasked to perform secondary missions, such as air-moving-target indication (AMTI) and geolocation. A DSS design maintains the capability to perform these multiple missions due to the inherent ability of the DSS architecture to reconfigure it's array geometry and baseline according to the requirements of each mission.

## **1.2 To Distribute or Not to Distribute**

Most agree that a variety of mission functions can be distributed across multiple satellites. Communication functions can be distributed across multiple satellites in LEO to minimize transmission latency, user handset power, is and constellation launch costs. Sparse aperture arrays can be comprised of formation flying satellite clusters. Multiple satellites provide favorable geometries for navigation. Less agreement found for distribution on the basis of enhancing the mission's architectural integrity.

In this area, the arguments for distribution are as numerous as the arguments against distribution. Those in favor cite decentralized resources enhancing survivability and reliability, smaller and simpler satellites being less expensive and lengthy to procure, modular design allowing upgradability, spatial distribution reducing revisit time, reduced range improving power-aperture product, manufacturing and testing economies of scale, use of smaller launch vehicles, lower failure compensation costs, etc. Opponents cite increased operations costs, minimal learning curve savings, risk associated with new technologies, complicated switching and communication logic, etc. What is clear is that while DSS provide a myriad of benefits and capabilities, it is not the panacea for all missions. It is essential that the answer to the question of "how much distribution is too much" be quantified early in the mission architecting cycle so that stakeholders are able to make informed decisions. This is the fundamental motivation for MIT's Generalized Information Network Analysis (GINA) methodology for Distributed Satellite Systems.

## **1.3 Developed Tools and Technologies**

To support this vision, the MIT Space Systems Laboratory undertook in-depth study of key areas within the field of Distributed Satellite Systems. While the following sections discuss the motivation, approach, and results in each of these areas, an overall roadmap is provided here. While the development of a quantitative systems architecting framework was the primary goal of this work, it was realized that several key technological enablers for distributed satellite systems needed to be developed and understood in order to conduct these architectural trades in a reliable manner. Therefore, the following summaries, as well as their companion sections, range from

system architecting tools, to sparse aperture physics, to satellite formation control, to lifecycle management, to mission studies and testbeds.

### **1.3.1 Generalized Information Network Analysis**

To answer the question of how much distribution is best, the Generalized Information Network Analysis (GINA) systems architecting methodology was developed [Section 2.1]. The GINA process identifies key physical attributes of a mission that need to be modeled to distinguish between candidate architectures, provides a framework for modeling these attributes in a lifecycle cost and performance context, and applies tools for searching and analyzing the architectural trade space using a set of comprehensive and quantitative metrics.

While the GINA methodology has been applied to numerous missions (Techsat21, Terrestrial Planet Finder, SPECS, GPS, MARS-NET, ionospheric mapper, broadband communication), Section 2.11 highlights the study of an operational follow-on to the Air Force Research Laboratory's Techsat21 space-based radar program.

### **1.3.2 Sparse Aperture Physics**

Understanding the physics of sparse aperture systems is essential to conducting architectural trades. Interferometric radar [Section 2.2] using the coherent integration of returns acquired by different satellites distributed in a half-kilometer diameter cluster was developed in support of the Techsat21 program.

For visible wavelength systems, signals cannot be recorded and integrated in a post-processing fashion. Instead, the light must be interfered in real-time. This places severe geometric constraints between the different collector spacecraft as well as with the spacecraft that is performing the interference. Satellite formation design, subject to these geometric constraints, is the topic of Section 2.3.

### **1.3.3 Satellite Formation Control**

To achieve and maintain the geometries required by the sparse aperture physics necessitates the use of several capabilities. Satellite clusters operating within a gravity well such as Earth's cannot afford the propellant needed to maintain a fixed geometry. Instead, orbits have been found that allow satellites within a local cluster to stay within the extent of that cluster with a minimal use of fuel [Section 2.4]. These orbits, a subset of Hill's Orbits, create a dynamic cluster as opposed to a static cluster because they cause the satellites to appear to orbit around each other. While such orbital solutions have historically been used for rendezvous maneuvers, this work uses them to create satellite clusters for sparse aperture systems.

A second capability is maneuvering of the satellites to reshape the formation. This can be used to alter the resolution of the sparse aperture or to allow the formation to perform some other mission thereby allowing the satellites to have multiple mission capability. Section 2.5 discusses methods for deriving optimum maneuver trajectories for reshaping satellite formations within Earth's gravity well.

A third capability is inter-satellite communication, command and control. The work summarized in Section 2.6 details the design and implementation of a real-time software architecture for formation flying satellites. This architecture accommodates acquisition of sensor data, estimation of satellite state, inter-satellite communication, execution of maneuver control, and telemetry to a ground station.

#### **1.3.4 Lifecycle Management**

Lifecycle management pertains to the study of the evolution of a distributed satellite system. The areas studied through this program included staged deployment, launch vehicle optimization, and end-of-life disposal. Since only soft interfaces (communication, metrology, control) couple the satellites comprising the formation, there is no need to launch all of the satellites in a formation at the same time. Instead, one could consider first launching the minimum number of satellites necessary to validate minimal mission functionality. This validation would improve confidence in the design, before all assets are launched, thereby reducing mission risk. In the event that a design flaw is discovered, the remaining launches can be grounded until a solution is found. Section 2.7 analyzes such a concept and extends it by also considering the ability to upgrade capability through subsequent launches.

When launching multiple satellites into a cluster or constellation, or replenishing the formation after satellite failures, one can consider optimizing the launch vehicle selection process. For example, one can consider cost as the driver and optimize the selection of a mixed fleet of launch vehicles to minimize launch cost. In addition, one can also consider risk. If a particular launch vehicle fails, that fleet will be grounded for some period of time until the cause has been identified and a solution has been implemented. This opens the possibility for optimizing a mixed launch vehicle fleet based upon launch delay risk. Section 2.8 summarizes work in this area.

By their very nature, distributed satellite systems present a space debris concern at the end of their lives. As a result, requirements have been defined for de-orbiting, or placing in graveyard orbits, satellites which have completed their mission or failed. Section 2.9 discusses techniques for disposing of distributed satellite systems.

#### **1.3.5 Mission Studies and Testbed**

Over the three years of the program, the MIT Space Systems Laboratory has developed application models, simulations, and testbeds for demonstrating, maturing, and applying the developed tools to missions of interest to the Air Force. Foremost among this mission set is the Air Force Research Laboratory's Techsat21 program. Following the successful completion of the Techsat21 technology demonstration flight experiment, the Air Force will most likely consider the possibility of a follow-on operation mission. However, such a mission will consist of a constellation containing a considerable number of satellites grouped into a number of local clusters. The performance and cost of such an operational system will be quite sensitive to the number of satellites, the size of the individual apertures, transmit power, orbital altitude, etc. Therefore, MIT applied the GINA methodology to the architecting of such an operational follow-on to Techsat21 [Section 2.10].



Key to the operation of these satellite formations is navigation, control, and autonomy. These technologies are quite immature and require extensive testing and refinement in representative environments in order to mature them to a level that makes them ready for flight. To this end, the MIT Space Systems Laboratory developed the SPHERES satellite formation flight laboratory [Section 2.11]. SPHERES consists of three nine inch diameter nano-satellites containing propulsion, communication, navigation, and control functionality. While SPHERES can be used in 1-g to test navigation, control and autonomy in two dimensions, it was designed for 0-g operation so that the full six degree of freedom dynamics of space can be used to mature these technologies. To this end, SPHERES is manifest for launch to the International Space Station on ISS-9a.1 in October 2002 where it will be used to mature formation flight algorithms. SPHERES will operate inside the Unity Module and have full access to (up)downlink channels, the crew, video coverage, etc. This dramatically reduces the risk typically associated with flight experiments since anomalous behavior can be quickly identified and rectified and depleted propellant tanks and batteries can be easily replaced. This feature makes SPHERES an ideal means for maturing high risk yet high payoff technologies.

The third application environment is the Generalized Flight Operations Processing Simulator (GFLOPS). Since soft interfaces play an essential role in coordinating the operation of these formations, the associated burden on inter-satellite communication and processing must be quantified and accounted for in the architectural trade process. In order to understand and minimize these burdens, MIT developed a regimented time, multiple processor simulation environment where the command and data handling features of a distributed satellite system can be rapidly coded and exercised in order to understand how to balance loads, resolve conflicts, and optimize throughput in these systems [Section 2.12].

## **2.0 TECHNICAL RESEARCH AREAS**

Section 1.0 was a brief overview of the Distributed Satellite Systems program at MIT. The following sections provide more in-depth summaries of the motivation, approach, results and future directions in each of the major research areas. Substantial documentation supports each of these areas in terms of theses, conference papers, journal articles, and design documents. This supporting material can be obtained from the Space Systems Laboratory by contacting the Director (David W. Miller) as specified below. This documentation is available individually or compiled on the DSS CD.

## **2.1 Generalized Information Network Analysis (GINA)**

### **2.1.1 Introduction**

Currently, the conceptual design of space systems tends to be unstructured, with designers often pursuing a single concept or modifying an existing idea rather than generating new alternatives. With such an approach, there is no guarantee that a systems level focus will be taken, and often the final design architecture chosen only achieves "feasibility" instead of "optimality." Systems level trades are often delayed until after a point design has been selected because of the perceived time and effort required to conduct a credible analysis. Further complicating matters

is the transition in the aerospace industry over the past decade from maximizing performance under technology constraints to minimizing cost with performance requirements. By not properly exploring the system trade space and thus not converging upon an efficient or even "optimal" solution during the conceptual design phase, the lifecycle cost of the system can greatly increase as modifications are required to properly integrate and operate the system during the latter stages of the design process, when design changes become much more expensive to implement.

GINA - the Generalized Information Network Analysis methodology for Distributed Satellite Systems (DSS) - is a systems engineering and architecting (SE&A) framework developed by the MIT Space Systems Laboratory. GINA enables the creation and comparison of numerous different design architectures for a given mission during the conceptual design stage. The foundation behind the GINA methodology is the belief that all satellite systems are information disseminators that can be represented as information transfer networks.

### **2.1.2 Approach**

A summary of the procedural steps in the GINA methodology is listed below.

1. Define the Mission Objective and the Conceptual Design Stage (CDS) Objective.
  - Identify the customer
  - State mission objective
  - Derive top level customer requirements
  - State CDS objective
2. Transform the Space System into an Information Network
  - Identify the origin-destination pairs in the network
  - Draw the network
  - Identify the 4 capability quality of service metrics
3. Develop System Metrics
  - Define the performance, cost per function, and adaptability metrics by which all proposed system architectures will be compared and evaluated
4. Partition the Problem
  - Define the design vector and constants vector
  - Matrix the design vector against the capability metrics
  - Define the modules
5. Develop Simulation Software
  - Develop each module
  - Code each module
  - Integrate the coded modules
6. Explore the System Trade Space
  - Evaluate the desired architectures on the basis of the system metrics
  - Apply an optimization algorithm if desired

Through these steps, GINA allows the systems engineer to make meaningful, quantitative trades at the conceptual design level by directly relating lifecycle performance to lifecycle cost.

### 2.1.3 Results

The GINA methodology has successfully been applied to a wide variety of missions, including the NAVSTAR Global Positioning System (GPS), commercial Ka-Band broadband communication systems, the Air Force TechSat 21 distributed radar concept for space-based ground moving target indication (GMTI), the NASA JPL Terrestrial Planet Finder (TPF), and the NRO Terrestrial Observer Swarm (TOS). In each case, GINA helped to organize, prioritize, and focus engineering effort; leading to a meaningful satellite systems analysis. In addition to enabling comparative analysis of different point designs for each mission, GINA served as the backbone for the application of multi-objective, multi-disciplinary design optimization (MDO) algorithms that can search the global trade space for the most cost effective system architectures.

Figure 1 illustrates the global trade space for the TPF mission. MDO methods coupled with GINA have been found to improve the conceptual design of distributed satellite systems by efficiently exploring the trade space of highly coupled problems for non-intuitive design solutions.

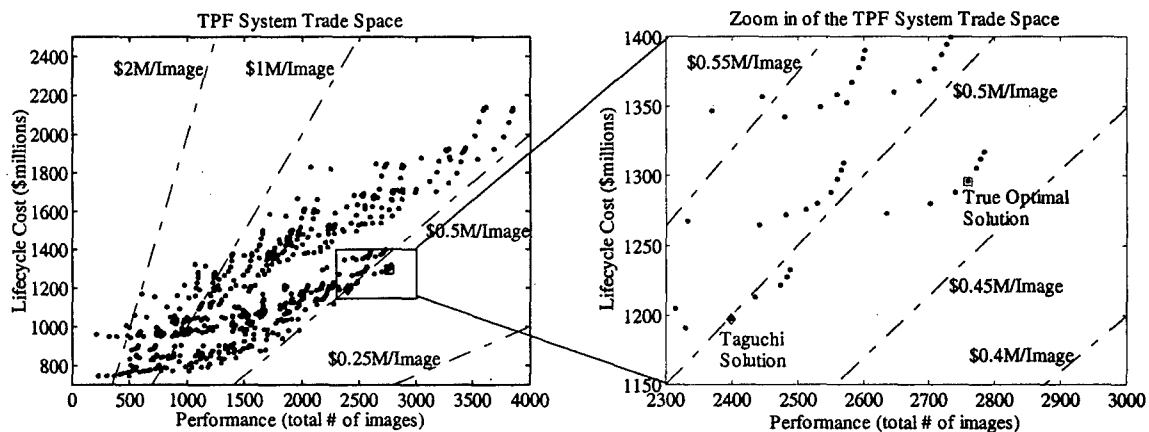


Figure 1. TPF Global Trade Space and Zoom-In of the Most Cost-Effective Region Within the Trade Space

### 2.1.4 Conclusions

In capturing the essential physics of all mission aspects, the GINA systems engineering methodology enables a comprehensive exploration of the conceptual design trade space for distributed satellite systems. By comparing architectures through comprehensive metrics based on information network theory, GINA produces more than single point designs – GINA actually helps find new cost effective design architectures. Coupled with MDO algorithms, GINA provides the system engineer with a tool to make, during the conceptual design stage of a program, intelligent architecture decisions that will directly impact lifecycle cost and performance.

## **2.2 Scanned Pattern Interferometric Radar**

### **2.2.1 Introduction**

Ground Moving Target Indication (GMTI) using separated spacecraft interferometry at radio wavelengths promises to be a powerful new all-weather surveillance tool. Our research is focused on the design of such a system, which is being developed as part of the Air Force Research Laboratory's (AFRL) TECHSAT21 program.

GMTI is typically used to locate large vehicles such as tanks and trucks in military applications. Current systems, such as JSTARS, use airborne platforms to provide temporary coverage in regions of interest. These systems provide good performance but are manpower intensive and require significant deployment time. Space-borne radar offers near continuous global coverage without appreciable operator risk.

The primary differences between air- and space-borne radar are the increased range and field of view. Increased range results in large signal attenuation from free space loss. In target detection radar, ground return obscures targets and is referred to as clutter. Increased field of view produces severe clutter, since a greater ground area is illuminated. As discussed in [1], there are three fundamental design considerations for space-borne radar. First, the radar requires sufficient power-aperture product to detect targets at the required search rate. Second, the angular and range resolution must be high enough to locate the target with the required degree of accuracy. Third, the radar must reject clutter and noise sufficiently to provide the specified probability of detection and false alarm rate. Thus, development of an effective space-borne radar system presents many challenges.

Single aperture systems are a compromise between high resolution and broad coverage. Broad coverage, or large field of view, requires a wide beamwidth, while high resolution requires a narrow beamwidth. In addition, clutter suppression is computationally intensive and requires prior knowledge of the target as well as an appropriate clutter model. Performance is therefore limited by the quality of prior target information and the accuracy of the clutter model.

In contrast, multiple aperture systems can provide coverage corresponding to the diameter of a single aperture, and resolution proportional to the maximum separation between individual apertures. Space-Time Adaptive Processing (STAP) has recently been proposed for use in multiple aperture systems [2]. STAP takes advantage of the high resolution properties of the interferometer, but does not use all the available information in the return signals. Like single aperture methods, STAP is limited by the accuracy of the clutter model.

### **2.2.2 Methods, Assumptions and Procedures**

TechSat21 is a technology demonstrator program with an experimental multiple aperture radar payload. It consists of clusters of microsatellites (less than 100 kg) that orbit in close proximity (on the order of hundreds of meters). Each microsatellite is capable of coherently detecting not only return signals resulting from its own transmission, but also return signals resulting from the transmissions of other satellites in the cluster.

Scanned Pattern Interferometric Radar (SPIR) combines the individual aperture signals in a way that allows ground clutter to be characterized completely and removed. This method depends not on the statistics of the clutter, but solely on the clutter position and Doppler shift. While the clutter amplitude and phase are random in nature, the Doppler shift is entirely predictable due to the known angular location of the clutter footprint. The algorithm relies on “de-convolving” the gain pattern of the synthesized aperture from the received signals to reveal the true ground scene.

In conventional interferometry, deconvolution is usually performed entirely in the spatial domain, and removes the artifacts that appear in the image as a result of incomplete (u, v) plane filling. SPIR uses the high angular variability of a sparse array Point Spread Function (PSF) to extract sufficient information from the signal return that the clutter and targets can be separated without an a priori assumption of the clutter statistics. Main lobe clutter can be separated from moving targets using the deterministic geometric relationship between observation direction and clutter Doppler shift. The algorithm synthesizes a PSF matrix corresponding to the gain pattern of the cluster as it is swept across the footprint. By deconvolving the synthesized gain pattern from the received signals the true ground scene is revealed.

#### **2.2.2.1      *A Simplified Model of SPIR***

A simple model of the SPIR approach is shown in Figure 2. The three boxes labeled RGB represent three footprint cells, which contain targets of unknown size. The array of arrows is the gain pattern associated with a sparse aperture with gains of 1,5,3,2 and 4. As the gain pattern is placed on the ground in a certain position, each of the gains multiplies the strength of the signal (radar cross section) from the corresponding cell. However, only the total signal strength is measured at the spacecraft. As shown, with the gains 3-2-4 covering the cells, the total signal strength is 27, whereas with 5-3-2 and 1-5-3 covering the cells, the total strengths are 26 and 20 respectively. With 3 samples taken (corresponding to the 3 unknowns) the problem can be formulated as a matrix equation, and provided the matrix is invertible, the values within R, G and B can be determined.

SPIR classifies each point on the ground according to its range, cross-range and Doppler shift. The Doppler shift of ground return is deterministically determined by the relative position and velocity between the ground and the satellite cluster and can be accurately predicted. Moving targets have a different Doppler shift from the ground they are on, and can therefore be efficiently separated from unwanted ground return, or clutter. The efficiency of clutter rejection is limited only by the ground and Doppler resolution of the system, and does not require prior assumptions about the nature of the clutter. Current radar interferometric systems require accurate clutter models in order to provide good clutter rejection.

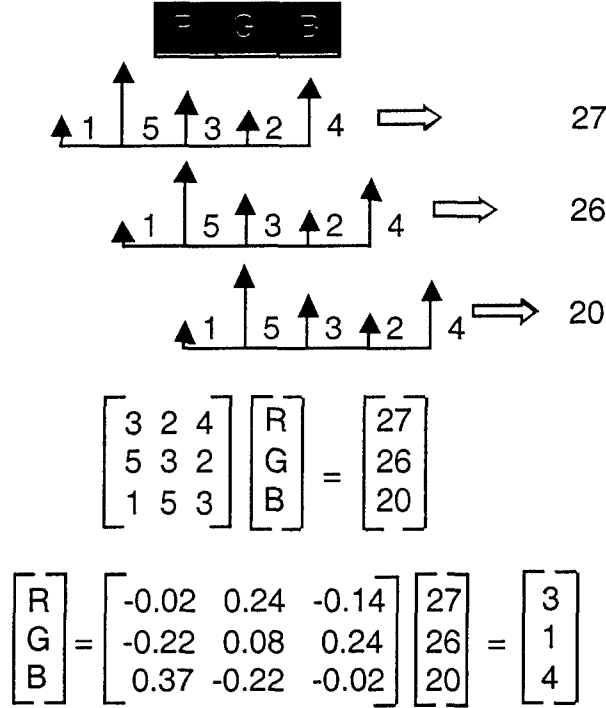


Figure 2. An Example of the SPIR Methodology [3]

## 2.2.3 Results and Discussion

### 2.2.3.1 The Mathematics of SPIR

The Point Spread Function (PSF) of an array is the gain pattern of the interferometer as a function of angle from boresight. For a two-dimensional interferometer with apertures at  $(x_i, y_i)$ , the PSF as a function of azimuth ( $\psi_a$ ) and elevation ( $\psi_e$ ) from boresight is

$$A(\psi_a, \psi_e) = \left[ E(\psi_a, \psi_e) \sum_{i=1}^{N_{\text{sat}}} e^{-\frac{j2\pi}{\lambda} (x_i \sin \psi_a + y_i \sin \psi_e)} \right]^2 \quad (2.2.1)$$

where  $E(\psi_a, \psi_e)$  is the response of the individual apertures. Figure 3 shows the PSF matrix for an array of eight satellites.

The SPIR algorithm relates the true ground scene  $x$ , expressed in terms of radar cross section (RCS) and Doppler shift, to the return signal  $y$  observed by an interferometer.

$$y = Ax \quad (2.2.2)$$

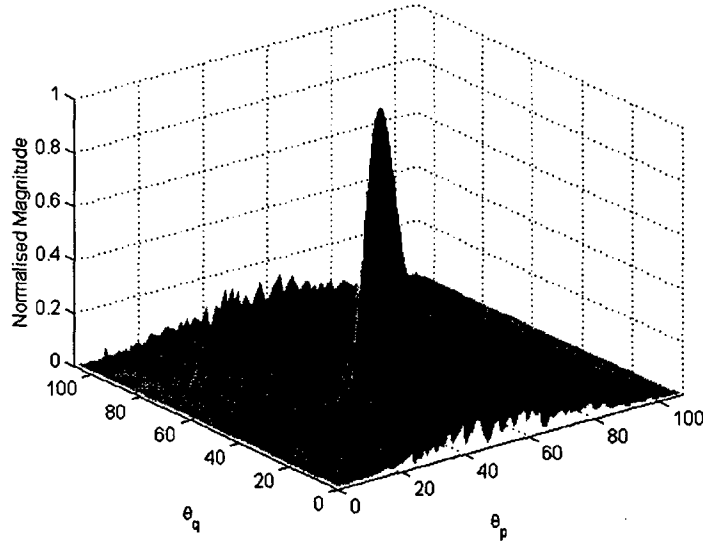


Figure 3. Point Spread Function Matrix for an 8-Satellite Unrestricted Array

The matrix  $A$  is referred to as the point spread function (PSF) matrix of the interferometer. In the case of a one-dimensional interferometer, the elements of  $A$  are defined by

$$A_{pq} = E(\theta_p) \sum_{i=1}^{N_{\text{sat}}} e^{-j2\pi \frac{d_i}{\lambda} (\sin \theta_p - \sin \theta_q)} \quad (2.2.3)$$

which is the PSF of the array, focused on a cell at angle  $\theta_p$  from boresight. For a complete derivation of the above results, see reference [4].

Figure 4 shows an example of a ground footprint at a single range recovered using SPIR. The two ridges are the ground clutter, while the two spikes are targets. Note that the targets are completely separated from the ground clutter.

### 2.2.3.2 Cluster Design

Success of the SPIR algorithm depends on the invertibility of the PSF matrix. In this research we develop design rules by which clusters that guarantee good performance can be designed. In the case of one-dimensional clusters, a design algorithm has been proposed, it is discussed in [4]. Future work will develop additional criteria with which to select particular irreducible arrays that provide the best system-level performance. Using such arrays the performance of SPIR in the presence of clutter and noise can be accurately estimated.

### 2.2.4 Conclusions and Recommendations

Space-based GMTI radar systems have the potential to achieve a high probability of detection for small, slow-moving targets. Current single aperture systems have produced exciting results, but the future lies with separated spacecraft interferometry. Constellations of multiple aperture

clusters will soon provide complete global coverage of potentially life-threatening developments around the world at lower cost and risk than current airborne systems. The design of such a system requires careful consideration of the signal processing used to combine a series of received radar signals to synthesize in the radar footprint.

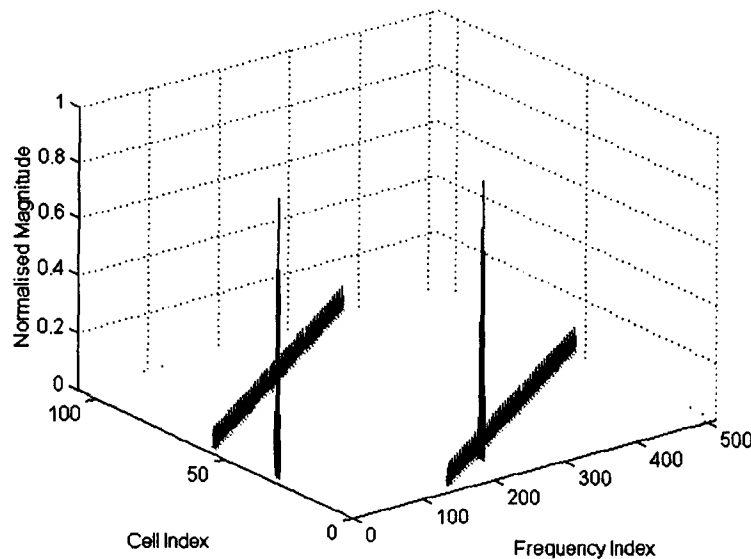


**Figure 4. Recovered Signal for a Footprint Strip with Two Targets**

One such method is SPIR, which provides near-ideal clutter rejection, albeit at some computational cost. With ever-increasing computational power, this should not place an undue burden on system design. One of the most significant advantages of SPIR is that performance is independent of the type of clutter.

## **2.3 Separated Spacecraft Imagers**

### **2.3.1 Introduction**

Systems employing a number of small satellites to perform functions that are traditionally achieved by a single monolithic spacecraft are becoming more commonly referred to as Distributed Satellite Systems (DSS). The many potential reasons for distribution, such as increasing survivability, coverage and reliability, have resulted in serious consideration in DSS by both the government (DoD and NASA) and the commercial sectors. One enabling technology brought forth by this distribution is the ability to synthesize much larger apertures than can be contained within a single deployment, providing significant increases in image resolution through interferometry.

To operate an interferometer in the visible or higher frequency regimes, signals from the collector spacecraft must be interfered in real-time, thus requiring a set of combiner optics. Not only must the signals be interfered, they must be coherently interfered at the same wave front, thus requiring the combiner optics to be located at the equal path length location. In addition to



this, a full axisymmetric angular resolution about the array's line-of-sight (LOS) is required such that a high angular resolution image of the target can be obtained.

This work is concerned with the orbit designs for a geosynchronous (GEO) separated spacecraft Earth imager operating in the visible regime. Two DSS architectures are considered, one of which involves the innovative exploitation of the properties of a circular paraboloid to meet the interferometric requirements. A comparison between the different DSS architectures for a visible Earth imager is then presented.

### 2.3.2 Methods, Assumptions and Procedures

The motions of the spacecraft in an array are best analyzed by considering their local movements as first order perturbations about some reference orbit. In general, this linearization is quite accurate since the size of the array is small compared to the size of the reference orbit. If the reference orbit is a circular Keplerian orbit, the resulting equations are simply the Hill's equations.

The simplest architecture is of course, to force all the collector spacecraft onto a circular trajectory and place the combiner spacecraft at the center of the circle. With this configuration, the line of sight of the array will be perpendicular to the trajectory plane since the target is in the array's far field. By centering the circular trajectory at the origin of the Hill's frame, no propellant is required for the combiner spacecraft. Thrust effort, however, is required to force the collector spacecraft to remain on the circular trajectory. The  $\Delta V$  required to hold a collector spacecraft in the circular trajectory as a function of the array's LOS is shown in Figure 5. From the figure, it is clear that there are preferential directions in which little effort is required to keep the spacecraft in the circular trajectory. In the case of the geo-synchronous Earth imager, the average  $\Delta V/n^2 R_o T_{life}$  required is approximately 1.55 units.

Rather than forcing the spacecraft into a forced trajectory, it is possible to place the collector spacecraft in an effort free trajectory. One solution the Hill's equations is an elliptical trajectory that projects a 2x1 ellipse in the  $x$ - $y$  plane and sinusoidal in the  $z$ -direction. Spacecraft that are placed in this ellipse should remain on this trajectory indefinitely. The equal path length requirement is met by considering the properties of a circular paraboloid. By fitting the ellipse onto an imaginary circular paraboloid, a combiner spacecraft placed at the focus of the paraboloid ensures that the reflected light rays from the target are coherently combined. In this case, the LOS of is in the direction perpendicular to the circle projected from the elliptical trajectory. As for the effort required to maintain the combiner spacecraft at the focus, the minimum  $\Delta V/n^2 R_o T_{life}$  required is 0.5672 unit (Figure 6).

To image off-nadir targets, delay lines must be introduced to the collector spacecraft such that off-nadir targets can be imaged. The length of the delay lines required is determined by considering the worst case scenario where the interferometer must be able to image targets from horizon to horizon. As a function of the array's LOS, the delay line length required is shown in Figure 7. The minimum delay line length required for the geo-synchronous Earth imager is  $0.31R_o$ .

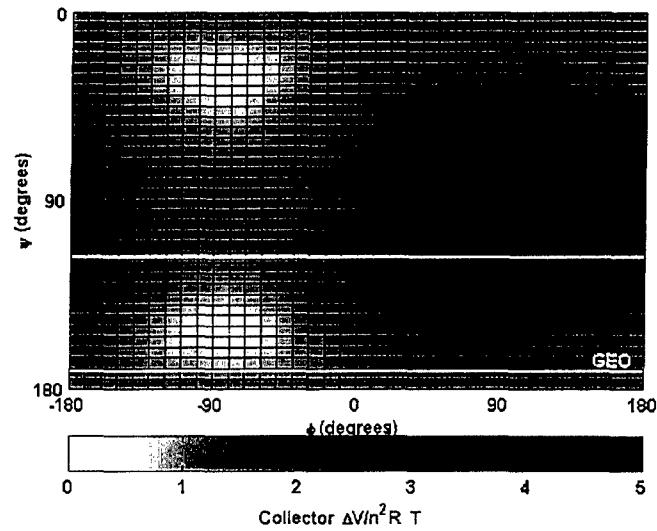


Figure 5. Variation of  $\Delta V/n^2 R_0 T_{\text{life}}$  as array's LOS is varied.

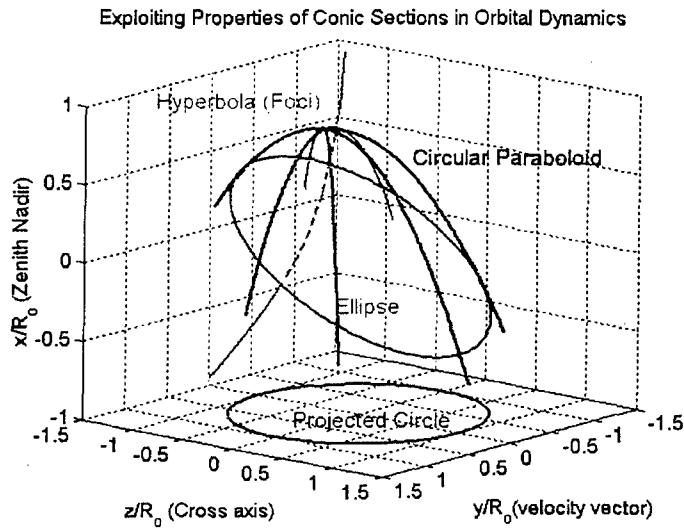


Figure 6. Exploitation of conic section properties in the second DSS architecture

The full axisymmetric requirement is met by considering both the locations and the size of the collector mirrors. Since the Cornwell imaging configurations were optimized for minimum redundancy in  $u$ - $v$  coverage, the task is then reduced to just determine the minimum aperture sizes required for the various numbers of apertures. Comparison of the fill factor of both the single frequency and broadband systems favor the use of broadband system. This is especially evident when the number of apertures in the system increases beyond five. The minimum aperture size required to provide full coverage for two different array size is shown in Table 1. Clearly seen from the table is the high optics mass required when only a small number of apertures are available.

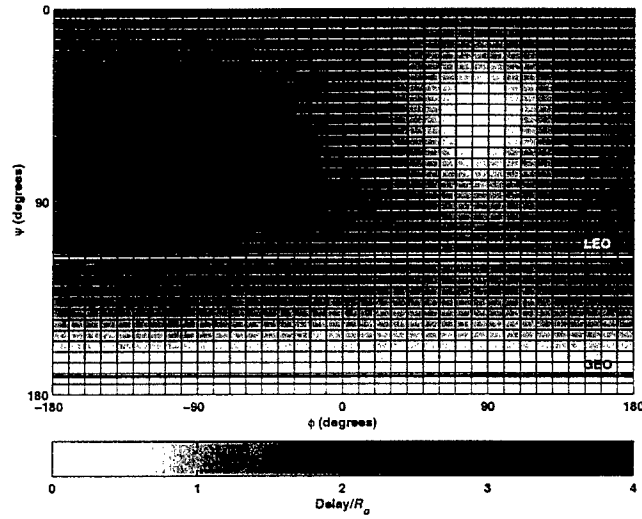


Figure 7. Delay line length required for imaging terrestrial targets

Table 1. Results using Cornwell Configurations for Broad Band Imaging

No of Points (n)	Aperture : Array (r/R <sub>0</sub> )	Aperture : Array (R/R <sub>0</sub> )	Arch. 1 (R = 8.50 m)			Arch. 2 (R = 9.30 m)		
			R <sub>0</sub> (m)	R (m)	Mirror (kg)	R <sub>0</sub> (m)	R (m)	Mirror (kg)
3	0.50	1.00	8.50	4.25	851	9.30	4.65	1020
4	0.38	0.95	9.00	3.42	551	9.84	3.74	659
5	0.29	0.95	8.95	2.60	317	9.79	2.84	380
6	0.20	0.99	8.59	1.72	138	9.39	1.88	166
7	0.18	0.90	9.44	1.70	136	10.33	1.86	163
8	0.15	0.96	8.90	1.34	84	9.74	1.46	101
9	0.15	0.99	8.63	1.29	79	9.44	1.42	95
10	0.12	0.93	9.19	1.10	57	10.05	1.21	69
11	0.11	0.89	9.55	1.05	52	10.45	1.15	62
12	0.10	0.99	8.59	0.86	35	9.39	0.94	42

### 2.3.3 Results and Discussion

Comparison between the two architectures is made based upon the total mass of each of the systems. The mass breakdowns of both the architectures are shown in Table 2. In the forced trajectory architecture (Architecture 1), the mass in the system are the combiner spacecraft, the collector spacecraft, the size of the mirrors and the propellant required to maintain the collector spacecraft's circular trajectory. As for the second architecture, mass contributors are the combiner spacecraft, the propellant required to hold the combiner spacecraft's position, the collector spacecraft, the collector's optics and the delay lines required for each collector spacecraft.

Comparison between the two architectures operating over a lifetime of 15 years favors the use of a six collector spacecraft using the forced circular approach (Figure 8). This minimum comes about from balancing the large optics required when few collector spacecraft are used and the mass of the collector spacecraft bus when more collectors are used. With a small array size ( $R_o = 8.5$  m), the propellant mass required to either maneuver the collector spacecraft or hold the combiner spacecraft stationary is not significant. A different trend, however, is observed when the size of the array is increased significantly ( $R_o = 25$  m). In this second case, the propellant mass begins to dominate the total mass of the system since more propellant is required to (1) hold the combiner spacecraft stationary (Architecture 2) and (2) ensure the more massive collector spacecraft remains on the circular trajectory (Architecture 1). Since the total mass is dominated by the mass of the collector optics, a drop of the mass as the number of spacecraft in the array is increased is observed.

**Table 2. Architecture mass contributing elements.**

Components	Architecture 1	Architecture 2
Combiner Bus & Optics	182.1 kg	182.1 kg
Combiner Propellant	-	$\Delta V/n^2 R_o T_{life} = 0.56$
Collector Bus	87.1 kg	87.1 kg
Collector Mirror	Table 2, Col. 6	Table 2, Col. 9
Collector Delay Lines	-	$0.31 R_o$
Collector Propellant	$\Delta V/n^2 R_o T_{life} = 1.55$	-

### 2.3.4 Conclusions and Recommendations

Imaging of terrestrial targets at resolutions that are beyond the capability of a single aperture is made possible with the advent of the interferometer. In this work, two trajectory designs that meet the requirements of a visible Earth imager using interferometric techniques were presented. In particular, an innovative trajectory design that exploits the properties conic sections while using optical delay lines to image off-nadir targets was also presented.

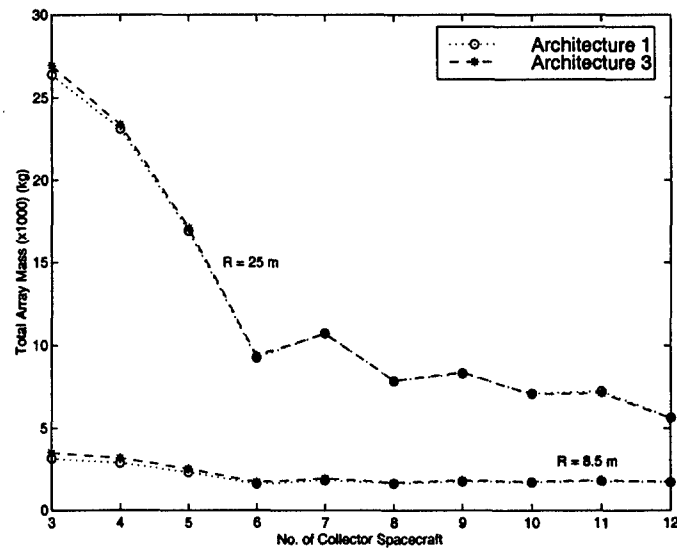


Figure 8. Total architecture mass as a function of number of collector spacecraft.

Comparison of the two architectures in terms of their total propellant mass indicates that the optimum imaging configuration for terrestrial imaging is to use a six collector spacecraft array while requiring them to follow the circular trajectory prescribed in Architecture 1. The results also indicate that the propellant requirement for the geo-synchronous Earth imager is rather small to affect the results. However, if the propellant requirement was found to be high, or when a large number of collector spacecraft are involved in the array, it seems to make more sense to use the free elliptical trajectories as determined in the second DSS architecture. This is due to the lower velocity increment required to hold the combiner spacecraft stationary.

The analysis used in this work can be extended to imaging stellar objects from within Earth's orbit. The difference in this case is to consider an inertially pointed system instead. Since it is more important to obtain high angular resolution images and not full coverage, the collector optics in this case are usually small. As such, comparison between the different designs should be dependent upon the propellant required to keep the spacecraft in formation.

## 2.4 Orbital Dynamics for Separated Spacecraft Clusters

### 2.4.1 Introduction

With the desire to place spacecraft into clusters of satellites, comes the need to accurately determine and control the position of each satellite within the formation. In order to accomplish this, researchers initially turned to Hill's equations. Hill's equations are a set of linearized differential equations that describe the relative motion of two spacecraft in similar near-circular orbits assuming Keplerian central force motion. Because these differential equations have constant coefficients, they have the ability to be solved analytically making them very useful.

In the past, Hill's equations have primarily been used for rendezvous maneuvers, but they have started to find a new use in satellite formation flying. Initial use of Hill's equations has proven useful, but they are limited by the assumption that the disturbance forces acting on the satellites

are negligible. The disturbance cited time and time again as preventing Hill's equation from being an effective tool for formation flying is the  $J_2$  geopotential. Because the Earth is an oblate spheroid, the gravitational potential is not constant as the satellite orbits the earth. This disturbance causes many variations over time in the satellite's orbital elements. These variations have a profound effect on satellite formations, and must be included in analysis of a satellite formation flying.

Some research still employs Hill's equations as their sole means of determining the satellite motion. Other research cites the errors in Hill's equations, primarily due to differential  $J_2$  forces, and determines the errors incurred by using them. Finally some research uses non-linear or numerical techniques to derive their solutions.

It has become apparent that a new set of equations are needed that are as easy to use as Hill's equations, but at the same time take into account the effects of the  $J_2$  disturbance force. At the MIT Space Systems Lab, we have done just that. A new set of constant coefficient linearized differential equations has been developed that incorporate the effects of the  $J_2$  geopotential disturbance.

#### **2.4.2 Methods, Assumptions and Procedures**

The derivation of the new linearized equations of motion are similar to that of Hill's equations. In Hill's equations, the zeroth order gravitational term is linearized with respect to a circular reference orbit. For the new equations, the  $J_2$  gravitational term is also linearized with respect to a reference orbit. While, in Hill's equations, the linearized gravitational term is a constant, the linearized  $J_2$  term is time varying. To fix this problem, the time average of the gradient of the  $J_2$  disturbance is used. This simplification allows for

Because the satellite in the cluster is now affected by the  $J_2$  disturbance, the satellites will drift away from the reference orbit since it is in an unperturbed circular orbit. Two changes to the reference orbit were required. The first was to match the orbital period of the reference orbit. This was accomplished by taking the time average of the disturbance force and applying it to the reference orbit. The second change to the reference orbit was to match the drift in the longitude of the ascending node. Under the influence of the  $J_2$  disturbance force, a satellite's longitude of the ascending node varies. The component of the  $J_2$  disturbance that is responsible for this drift is the component of the  $J_2$  disturbance that is normal to the orbital plane. This component was added to the reference orbit, and thus the reference orbit now remains in close proximity to the reference satellite.

Each component of the  $J_2$  disturbance that was added to the reference satellite is now subtracted from the relative equations of motion. This results in a set of constant coefficient, linear, differential equations of motion that can be solved analytically.

Due to the time averaging of the gradient of the  $J_2$  disturbance, the new linearized equations of motion fail to capture the cross-track motion correctly. This was corrected by using spherical trigonometry and the mean variations in the orbital elements.

The final solutions to the equations of motion of one satellite relative to another are shown below.

$$\begin{aligned}
 x &= x_0 \cos(\sqrt{1-s} \, n t) + \frac{\sqrt{1-s}}{2\sqrt{1+s}} y_0 \sin(\sqrt{1-s} \, n t) \\
 y &= -\frac{2\sqrt{1+s}}{\sqrt{1-s}} x_0 \sin(\sqrt{1-s} \, n t) + y_0 \cos(\sqrt{1-s} \, n t) \\
 z &= A(t) \left( \frac{z_0}{A(0)} \cos(B(t) \, t) + \frac{\left( \frac{\dot{z}_0}{n\sqrt{1+3s}} \right)}{A(0)} \sin(B(t) \, t) \right) \\
 \dot{x}_0 &= \frac{n y_0 (1-s)}{2 \sqrt{1+s}} \quad \dot{y}_0 = -2 n x_0 \sqrt{1+s} \\
 \text{where} \\
 s &= \frac{3J_2 R_c^2}{8 r_{ref}^2} (1 + 3 \cos 2i_{ref}) \\
 A(t) &= r_{ref} \Phi(t) \\
 B(t) &= n\sqrt{1+s} - \frac{\Delta\gamma}{t}
 \end{aligned}$$

### 2.4.3 Results, Verification and Discussions

Two methods were used to verify the validity of the new linearized equations of motion. First, the solutions to the linearized equations of motion were compared to the mean variations in the orbital elements. The solutions to the new linearized equations of motion were able to capture the mean variations in all six of the orbital elements.

Second, a numerical simulation was used to verify the solutions of the linearized equation of motion. A cluster with no drift from the reference orbit has 4 initial conditions that can be independently varied. Each of the 4 initial conditions was varied independently and the remaining initial conditions were set such that there was zero secular drift. The solutions to the linearized equations of motion had periodic errors that were less than 0.2% of the overall cluster size. This is a marked improvement over Hill's equations which have errors that increase considerably over time. Shown below are the results of one numerical simulation. A satellite with an initial offset off 100 meters in the radial direction produces the following errors in the three orthogonal directions (radial, in-track, cross-track). As shown below the maximum error here is 6 centimeters, or 0.06%, in the cross-track direction.

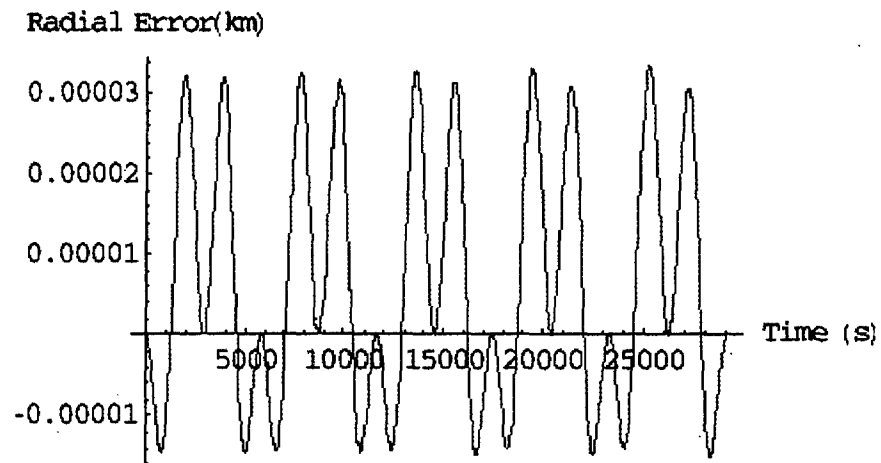


Figure 9. Radial Error (m) of Estimated Position Over Time

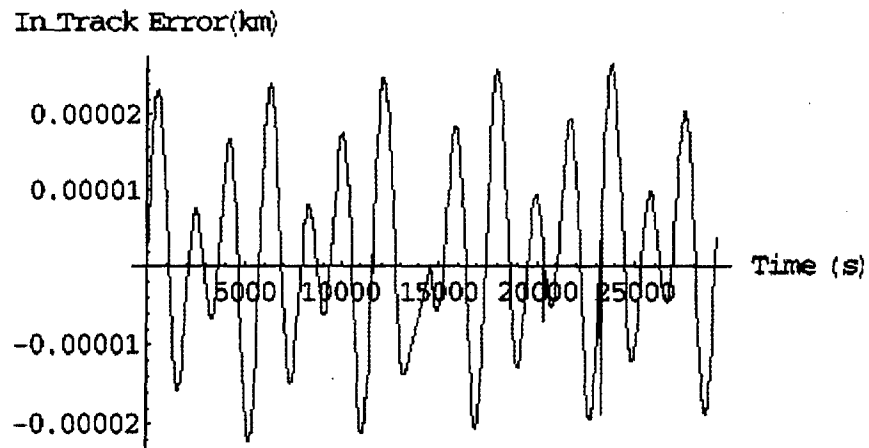


Figure 10. In-Track Error (m) of Estimated Position Over Time

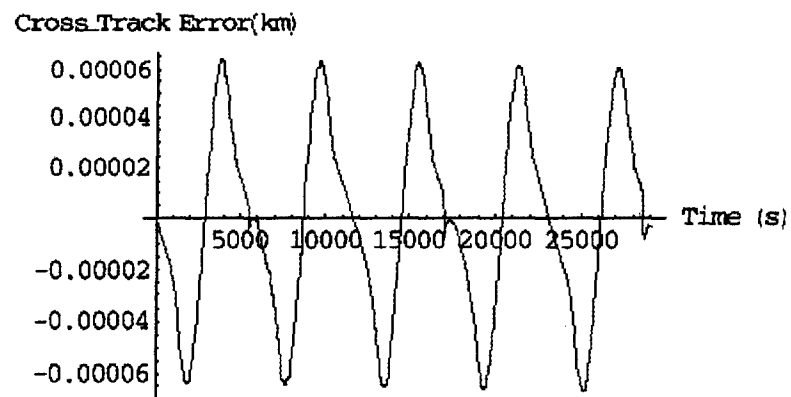


Figure 11. Cross-Track Error (m) of Estimated Position Over Time



With the creation of these equations, some insight has been gained into the effect of the  $J_2$  geopotential on formation flying. One effect is called 'Tumbling'. Tumbling is the result of a difference in periods between the in-plane and out-of-plane motion of a satellite in the cluster. This motion causes the cluster as a whole to 'tumble' about the axis normal to the orbital plane. It should be noted that this motion is not a differential  $J_2$  effect. In other words, if each satellite sees the exact same disturbance force, this effect still happens. For missions that require specific projections of the cluster geometry, tumbling will be an effect of the  $J_2$  disturbance that must be compensated for. This can be done with active control at a cost of propellant, or by overpopulating the formation so that the projection never degenerates.

Another effect of the  $J_2$  geopotential is the tendency for satellites in a cluster to separate due to differential disturbance effects. Because each satellite does not see the exact same disturbance force, each satellite has slightly different motion. Differential  $J_2$  effects cause different variations in the longitude of the ascending node. This variation, along with a geometric effect called scissoring, causes the satellites in the cluster to drift away from the cluster origin. The variation also causes the intersection of the orbital planes of the satellites to move towards the poles. Therefore, differential  $J_2$  affects both the size and shape of the satellite cluster.

#### **2.4.4 Conclusions**

A new set of linearized equations of motion have been developed for satellite formation flying. These equations of motion are similar to Hill's equations in the form and ease of use, but at the same time capture the effect of the  $J_2$  disturbance force. The development of these equations of motion brings insight to satellite cluster dynamics and provides a tool for developing trajectory optimization and control algorithms.

### **2.5 Formation Flight Maneuver Optimization**

#### **2.5.1 Introduction**

Significant advantages observed in distributed computing environments, such as improved overall system reliability, cost and coverage, have led to functions that were traditionally performed by a large monolithic spacecraft to be distributed among clusters of smaller and more cost effective spacecraft. When appropriately utilized, these spacecraft have the potential to perform significantly better than their traditional counterparts. This distribution, however, does come at a cost. Even though significant cost advantage may be exploited with the construction of many smaller spacecraft, operational complexity multi-spacecraft fleets is significantly increased. One such complexity is the coordination of the spacecraft motions relative to each other to avoid collisions while minimizing the resources.

Previous work in this area has been to minimize the propellant required to re-configure an array. These optimizations are useful for low specific impulse systems where propellant expenditures are rather significant. With significant technological advances in high specific impulse electric propulsion, more missions are beginning to adopt such systems for both station keeping and orbit transfer maneuvers. As such, determining trajectories that minimizes propellant usage for these spacecraft may not be appropriate.

The lack of work in formation flight maneuver optimization based upon an energy metric prompted this investigation. Using the approaches developed in the field of optimal control theory, minimum energy trajectories for Earth orbiting clusters are determined. Results specific to initializing and re-sizing the Air Force Techsat 21 cluster are then presented. Finally, the conclusion and further recommendations of the work are presented.

### **2.5.2 Methods, Assumptions and Procedures**

The approach taken in this formation flight maneuver optimization is based upon the calculus of variation technique. Originally developed in the field of optimal control, this technique is suited for trajectory optimization. To utilize this technique, two key components must be specified; (1) the dynamics of system and (2) the objective function of the problem. Given these components, the technique then allows for the control law to be developed such that a trajectory that minimizes the objective function can be determined.

Since the case study for this work is the Techsat 21 mission, the dynamics of the system is simply the motions of the spacecraft with respect to one another under the influence of Earth's gravity. These motions can be best treated by considering the spacecraft local movements as perturbations about some reference orbit. Using this approach, a set of linearized second order differential equations of the spacecraft dynamics was developed by Hill.

The attractiveness of high specific impulse offered by the electrical propulsion system have led to the selection of Hall Thrusters for the Techsat 21 spacecraft. As with high specific impulse system, little propellant is consumed over the lifetime of the system. The emphasis in using this propulsion system is to minimize the electrical power required to operate the thrusters. Since the electrical power required is a quadratic metric, the objective of the optimization is to determine the trajectories that would minimize the electrical energy required. With linear dynamics and quadratic objective function, it can be shown that the optimal controller is indeed the Linear-Quadratic (LQ) controller. Since the LQ problem is a classic modern control problem, there exist many tools to tackle the problem at hand.

To determine the optimal cluster trajectories, it is important to determine the final destination of the spacecraft. Previous work in this area found that the homogeneous solution to the Hill's equation describes an elliptical trajectory in the Hill's frame. Spacecraft placed in this ellipse trajectory should not drift apart. As such, this elliptical trajectory is ideal for spacecraft formation flight since no effort is required to ensure that the spacecraft remain in a close formation with respect to each other. In a multi-spacecraft mission, it is also important to ensure that the spacecraft phased correctly. Rather than using an angular separation metric, a relative distance metric was developed to account for this phasing requirement. The angular phasing of the spacecraft were converted into distance requirements and used to check the spacecraft terminal states. The distance metric was found to be simpler to use compared to the angular separation metric since it was not necessary to deal with any inverse trigonometric relations.

### **2.5.3 Results and Discussion**

Minimum energy trajectories for a cluster of  $N$  spacecraft as a function of initialization time were determined. The results indicate that the relatively high levels of electrical energy are required

when short initialization times are allowed. The energy levels, however, decrease quite significantly if the initialization time is increased to beyond one period. It was also observed that the average energy levels required is strongly dependent upon the length of initialization time, and not on the number of spacecraft in the cluster (Figure 12).

The maximum power that is currently available to the Techsat 21 is 200 W. As such, it is important to ensure that the minimum energy trajectories do not require instantaneous power level beyond that is available to the spacecraft. As in the case with the energy levels required, the instantaneous maximum power required was found to high when short initialization time is allowed. In the case of the Techsat 21 mission, it was found that the spacecraft can be initialized to the desired configuration only if the initialization time is increased to beyond 0.2 orbital periods (Figure 13).

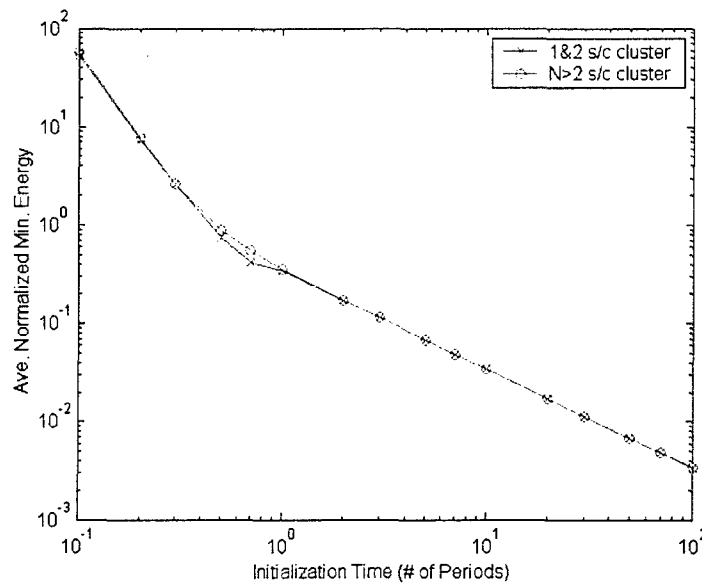


**Figure 12. Average energy required per spacecraft to initialize a cluster of  $N$  spacecraft**

The velocity changes ( $\Delta V$ ) expended as a result of following the minimum energy trajectories were also determined. As with both the energy and power levels required, the  $\Delta V$  required decreases with time. Significant  $\Delta V$  is needed when short initialization time is allocated. This allows for up to 67% in  $\Delta V$  savings when the initialization time is increased to beyond one orbital period (Figure 14).

The objective in the re-sizing problem is to increase the size of the cluster such that a higher angular resolution can be achieved. One such application is to locate pilots that have just ejected from their planes. As far as the power requirement is concerned, a minimum of 36 minutes of re-sizing time must be allocated such that the cluster can be re-size to the required 2.5 km baseline (Figure 15). In terms of the  $\Delta V$  required, it was again found that significant  $\Delta V$  is required when only a short re-sizing time is allocated. However, the  $\Delta V$  asymptotes to a value of 10 m/s when the re-sizing time is increased to beyond one orbital period. This  $\Delta V$  is considered quite significant as only 40 m/s of  $\Delta V$  is currently budgeted for the flight experiment spacecraft (Figure 16).

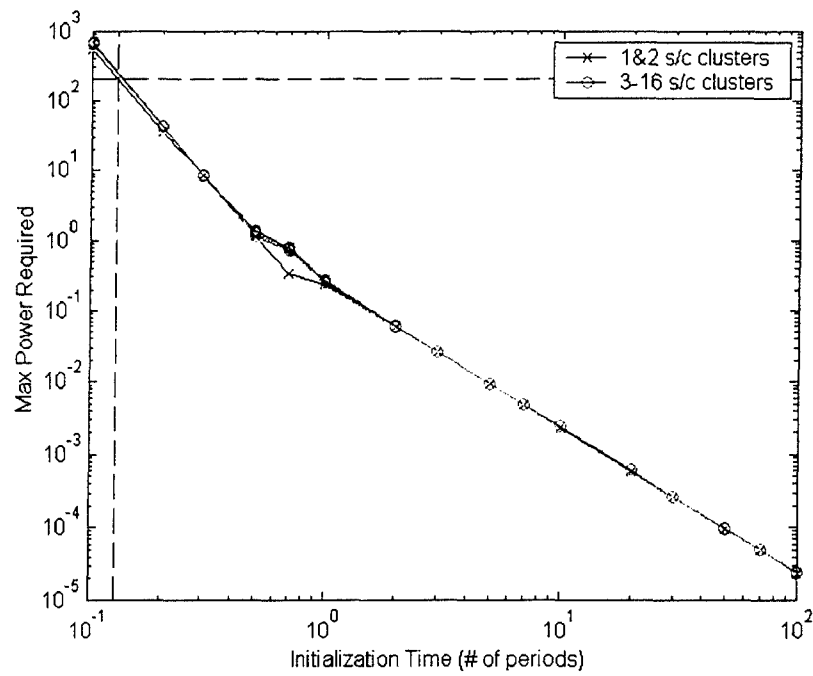


Figure 13. Maximum power required to initialize a cluster of  $N$  spacecraft

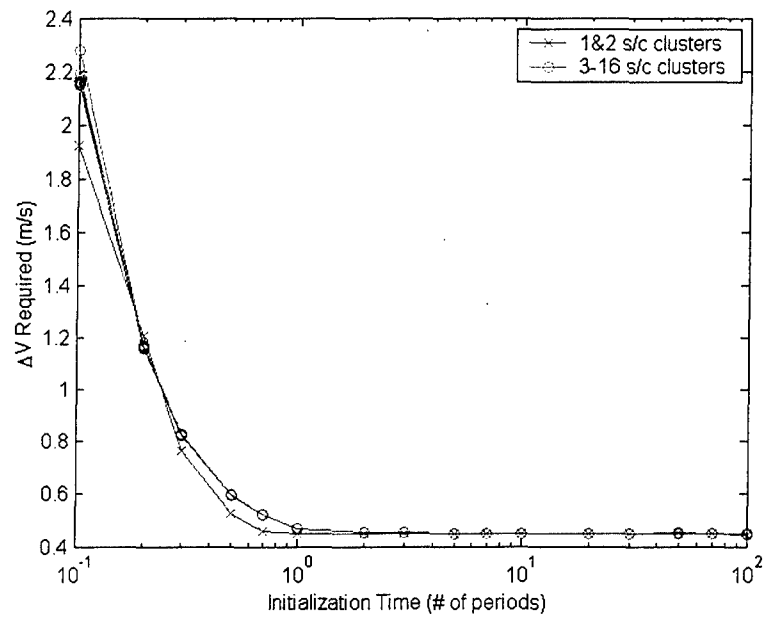


Figure 14. Average  $\Delta V$  required per spacecraft to initialize a cluster of  $N$  spacecraft

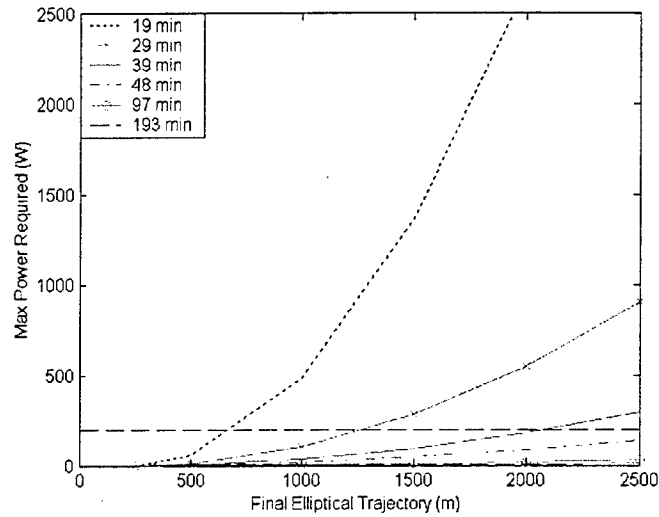


Figure 15. Maximum power required to re-size the Techsat 21 cluster

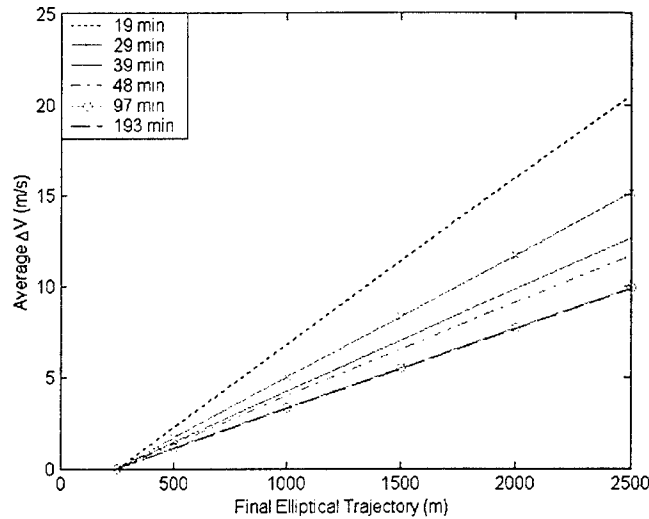


Figure 16. Average  $\Delta V$  required to re-size a cluster of 3 spacecraft.

#### 2.5.4 Conclusions and Recommendations

In this study, an algorithm to determine the optimal trajectories to re-orient a cluster of spacecraft has been developed. The problem, framed as an optimal control problem, was solved using the well known linear-quadratic controller, namely a system with linear dynamics and quadratic costs. Terminal constraints geared towards the Techsat 21 mission were also developed.

Cluster initialization and cluster re-sizing results specifically for the Techsat 21 flight experiment were presented. In the initialization problem, it was determined that the cluster can be initialized in as little as half an orbital period. However, one may consider increasing the initialization time as up to 67% of  $\Delta V$  savings can be achieved. In the minimum energy trajectories, it was also found that the bulk of the effort was spent on changing the spacecraft orbital inclination. In the re-sizing problem, maneuvering times of less than 0.4 orbital periods are not possible for the

flight experiment spacecraft to re-size to an elliptical trajectory of 2.5 km. In cases where the cluster can be re-sized, significant  $\Delta V$  is required. It was also found that by increasing the maneuvering time beyond one period, the velocity required to re-size the array remains almost the same.

The methodology developed in this study can also be applied to other multi-spacecraft missions. One example, is the NASA's Space Technology 3 two spacecraft visible interferometer. Optimal trajectories for the two spacecraft outside of the Earth's gravity well can be determined using a combination of energy and imaging metrics. A further possibility is to determine the optimal trajectories for a stellar imaging interferometer operated within the Earth's orbit. Should it be feasible to operate a separated spacecraft interferometer within the Earth's orbit, significant savings in both launch cost and operational cost can be achieved due to the spacecraft closer proximity to Earth.

## **2.6 Micropropulsion System Selection for Precision Formation Flying Satellites**

### **2.6.1 Introduction**

Several of NASA's upcoming scientific interferometry missions (ST-3, LISA, TPF, etc.) are pushing the limits of precision positioning of satellites. These spacecraft will require position and attitude control actuation on exceedingly small scales, which has not previously been performed. The several candidate propulsion systems for these missions include: colloid thrusters, field emission electrostatic propulsion thrusters (FEEP), pulsed plasma thrusters (PPT) and miniature cold gas thrusters. In order to assess the appropriateness of each of the candidate micropropulsion systems, a model of each is constructed. The models created are conglomerations of basic physical concepts and empirically founded relationships. Emphasis is placed on the determination of key operating parameters that are most relevant to the systems level of design. Along with models of propulsion system performance, a common set of metrics is defined to allow varied concepts to be compared fairly. High-level propulsion system design has been performed for each mission, employing the propulsion models created. These designs are evaluated according to the metrics developed and judgments about the most useful requirements for which to use the different propulsion systems are made.

### **2.6.2 Methods, Assumptions and Procedures**

Five interferometric space science missions were investigated and their requirements were flowed down to constrain the propulsion system designs. The missions used were Space Technology 3 (ST-3), Terrestrial Planet Finder (TPF), Laser Interferometer Space Antenna (LISA), Micro-Arc-Second X-ray Interferometry Mission (MAXIM) and Submillimeter Probe of the Evolution of Cosmic Structure (SPECS). Some of the most influential design requirements and specifications include mission lifetime, orbit, position accuracy requirements, maximum drift speeds and disturbance spectral signatures.

The metrics, integrity and cost, are a distillation from the GINA methodology and were used to evaluate the overall performance of the propulsion system designs. The integrity derivative

comes from the modeling of the control and actuation characteristics of the propulsion systems, while the modified cost metric is dictated more by the propulsion system physics.

In the context of missions whose science objectives employ interferometry to acquire a signal, the integrity metric can be affected by anything that degrades the signal quality. Therefore, the integrity metric can be thought of as how well the spacecraft's position and attitude can be maintained. This kind of stationkeeping or formation flying accuracy often determines the level of confidence that can be attributed to the mission data gathered.

The impact on cost that a particular propulsion system design has on the overall system was measured by two attributes. The first is a mass value, which takes into account the effects of actual propulsion system mass and relative changes in the mass of other spacecraft components caused by the propulsion system design. The other attribute is a technology readiness level rating as defined in the standardized system used by NASA. This rating indicates how close a given technology is to maturity, in the sense of space flight readiness.

For the purpose of creating a single cost metric for each mission, a dollar value is attributed to each kilogram of hardware. The dollar value is based on both launch costs and hardware manufacturing costs. The hardware manufacturing costs are based on theoretical first unit costs (TFUs) that are described in [5] as function of hardware mass. In order to construct technology development cost estimates, information from a NASA memo [6] and a recent NASA Technology Announcement [7] were combined to create a relationship between the current TRL of a technology and the amount of money in current dollars required to bring the TRL of the technology to flight readiness.

A model was created for the analysis of each propulsion system. The four propulsion systems (colloid thrusters, FEEP thrusters, PPTs and cold gas thrusters) were modeled by combining the most salient and tractable features of their underlying physics with the characteristics that make them unique in terms of flexibility and methods of actuation and control.

The PPT model simulates the thruster's ability to maintain position in an environment with a constant or time varying disturbance force. Various thruster parameters can be adjusted to meet the performance specifications of the mission. The tunable parameters in the PPT model include the disturbance profile and magnitude, the impulse bit, the maximum PRF, the dead-band distance requirement and the simulation duration as well as the spacecraft mass. They in turn determine important system metrics like average and peak power consumption, propellant usage and thruster size, as well as thrust profile, trajectory and position and acceleration PSDs.

The colloid thruster model captures the aspects of 'controlling' the thruster in addition to representing some physical characteristics of the colloid thruster operation. The thruster unit has two levels of thrust control. The coarser level determines how many needles are emitting and the finer level determines the depth of the potential the droplets are accelerated through. The system can therefore be designed in such a way as to create continuous throttling capability through a range of thrusts far exceeding that of a single needle. The control is designed to nullify the impulse imparted to the spacecraft by the disturbance force and to keep the spacecraft at the specified position. A disturbance profile is specified and it, coupled with logic to control the

switching of the various blocks and the accelerator voltage, is used to produce a thrust profile, a trajectory and PSDs of both position and acceleration.

The FEEP system is a continuously throttleable propulsion unit with no known non-idealities, aside from a small steady-state noise. However, the frequency content of this noise was not available. So, the FEEP model uses data available from tests performed on the indium FEEP to capture the effect of this noise. It is not incorporated directly into the simulation, only used as a reference afterward to guide performance evaluations. An effort was made to construct the FEEP model to be as similar to the other models as possible to allow for a meaningful comparison among them. Therefore, the disturbance force has the ability to be varied in the same ways as the other models and the metrics like power, mass, thrust profile, trajectory and PSDs of position and acceleration are provided.

The cold gas thruster operational model is similar to the PPT model in that the major mode of operation is in the pulsed regime. The method of pulsing cold gas thrusters is somewhat less restricted than that of a PPT, however. While, in general, a specific cold gas thruster has a single thrust magnitude, the pulse width is not fixed as it is with a PPT. Therefore, the pulse width is another parameter, in addition to PRF, that can be varied to match a disturbance force more accurately.

Next, a compilation of preliminary designs for each propulsion system-mission combination was created. Table 3 shows a list of the major parameters for the propulsion systems designed for the SPECS mission and Figure 17 shows the relative costs of those propulsion systems as determined by the metrics developed.

**Table 3. SPECS Propulsion System Designs Summary**

<b>Metrics</b>	<b>PPT</b>	<b>Colloid</b>	<b>FEEP</b>	<b>Cold Gas</b>
Fixed Mass [kg]	42	15.63	35.43	0.36
Variable Mass [kg]	9.39	13.32	0.66	757.56
Mass Fraction (%)	13.7	7.7	9.6	202
Normal Power [W]	0.89	0.17	2.39	3.8
Maximum Power [W]	35.52	0.43	2.67	10
Solar Array Mass [kg]	1.07	0.013	0.081	0.3
TRL	7	3.5	5	6.5
$\Delta x$ [m]	$5 \times 10^{-6}$	$1 \times 10^{-12}$	$1 \times 10^{-11}$	$5 \times 10^{-6}$



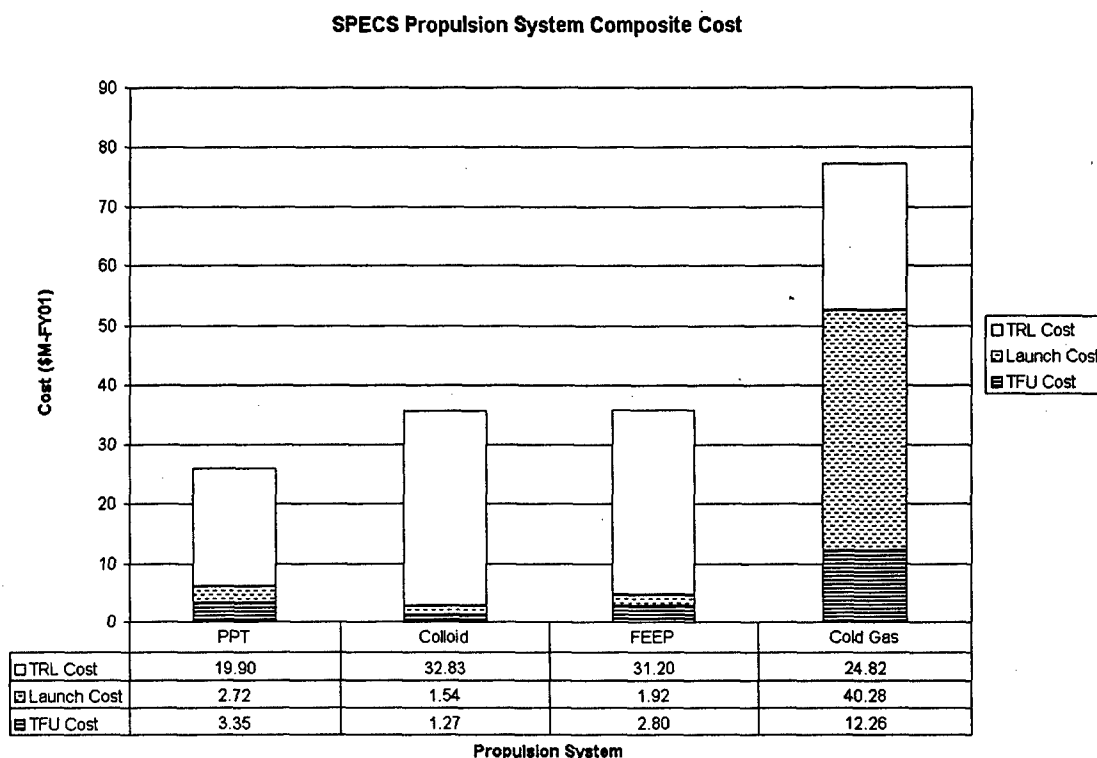


**Figure 17. SPECS propulsion system total costs including development, hardware and launch.**

### 2.6.3 Results and Discussion

The propulsion system designs are evaluated according to the aforementioned metrics, resulting in a best propulsion system for each mission and general trends discovered throughout the trade space. A summary of the propulsion systems that were selected as the best choice for each mission, based on both the compiled cost estimates and the issues mentioned in the selection and trades discussions, are listed in Table 4. The selections are provided for both the short term and long term perspectives. The short-term perspective shows that the PPT system dominates the selections likely in large part due to the fact that it is the most highly developed system with a high performance specific impulse. However, there are niches in the design space where each of the propulsion systems seems to be preferable. Additionally, there are a few cases in which there are several propulsion systems that can meet the mission requirements efficiently. Particularly, the similarity between the FEEP and colloid systems in cases where the  $\Delta v$  requirements are not extremely large and there are not a large number of thruster units required. Regardless of the details, it does appear that both the colloid and FEEP thruster systems have applications in several of these precision formation flying missions and therefore warrant further development.

**Table 4. Propulsion System Cost-Based Selection Summary**

<b>Perspective</b>	<b>ST-3</b>	<b>TPF</b>	<b>LISA</b>	<b>MAXIM</b>		<b>SPECS</b>
<b>Short Term</b>	PPT	PPT	Colloid/ FEEP	Colloid/CG	PPT	PPT
<b>Long Term</b>	CG	FEEP	Colloid	Colloid/CG	FEEP/Colloid /PPT	Colloid/FEEP

### **2.13.1 Conclusions and Recommendations**

The selection of the precision formation flying propulsion systems for the five missions examined in this study is based on three major criteria. They include performance, cost and technical feasibility. Performance is judged by the ability to meet specified mission requirements. Cost is based on hardware manufacturing, launch and necessary research and development. While not included quantitatively, the technical feasibility of developing a propulsion technology is discussed and used to influence the recommendation of propulsion systems for implementation on the missions. It is shown that all of the propulsion systems examined have potential areas of usefulness. Additionally, it is seen that the extent of technological development of a propulsion technology can have a large impact on the financial resources necessary for its implementation on a given mission.

There are several areas in which this work can be expanded upon or refined. Of particular importance to interferometric missions appears to be the issues associated with detector contamination. Another potential area for more detailed work lies in a rather different topic. In order to further verify and validate the results gleaned from the propulsion system operational modeling simulations, it is felt that control algorithms similar to the type that would actually be used for the spacecraft control system should be integrated with the propulsion system characteristics (often described as models of actuator transient dynamics). This modeling, in conjunction with more data on the steady state behavior of the propulsion systems, could provide more authoritative and trustworthy results.

## **2.7 Software Architecture for Satellite Formation Flight**

### **2.7.1 Introduction**

The goal of formation flight algorithms is to provide better accuracy than that possible by independent satellite constellations. To accomplish this, formation flight algorithms use differential measurements to provide the accuracy necessary for missions that require separated spacecraft to behave as a single, larger spacecraft. These systems, though, have higher computational and communication requirements than those of standard real time systems. The software retains the basic framework of a real-time environment (a fixed rate interrupt runs a controller, and housekeeping tasks are run in a background process). But a distributed satellite system will require several additional processes in order to accommodate multiple rate processors, asynchronous communications and control, and synchronization methods. How the system addresses these issues depends on the interconnection architectures.

### 2.7.2 Methods, Assumptions, and Procedures

The studied formation flight architectures are: independent units, master/slave, leader/follower, and peer-to-peer control. The independent units tests are used as the base case. In this case all the units operate independently of each other, using regulation controllers to maintain an absolute position. If this absolute position were maintained perfectly, the units would stay in formation. But these absolute positions may not provide the desired accuracy for the system as a whole; further, they are highly affected by disturbances to individual satellites.

The simplest Formation Flight control scheme is a Master/Slave architecture. In this scheme, the Slave does not perform any decisions, it simply follows the Master blindly so as to keep the desired formation. Overall, the Slaves are sensor/actuator pairs; the Master performs all the calculations to maintain formation of the system. This scheme allows the formation to be modeled as one single unit. This assumption greatly simplifies the modeling of the FF system: moving the Master correctly will move the formation correctly. The master/slave systems use high bandwidth communications and low powered processing units. They do not implement any redundancy or global knowledge of the system's state.

Two types of controllers are considered for the master/slave architecture: local and global. Local controllers perform the command computations within the slave and master units. They require the state of the master to be transmitted as fast as possible to the slaves, so that they can follow, but not necessarily in real time. Global controllers reside solely in the master unit. These controllers use information from the slaves and transmit the commands themselves. This requires high bandwidth, high reliability, real-time communications. Due to the expanded size of the state vector, they will require higher computational power in the master unit.

While a slave is a dumb entity, a follower has knowledge of the complete formation, and therefore can perform decisions without the intervention of the leader. Under this scheme the leader still acts as the hierarchical center of the formation. The leader is the main reference for the formation, and the followers move around it. Yet, if the leader stops operating or is sent far from its formation, the followers will not stop functioning or move far from formation. In the cases of catastrophic failure of the leader, one of the followers can take its place, and the formation would be centered around the new leader. If the leader moves far out of formation, the followers may decide not to follow and wait for the leader to come back into formation. Such an action would save power and propellant among the followers. The leader/follower scheme trades processing power to obtain the redundancy missing in a master/slave system.

In a peer-to-peer network all the units are at the same hierarchical level. This idea combines the independent unit scheme with the leader/follower scheme. The ground station commands all units to perform a certain formation. With this goal specified, the units independently start to move to formation; yet, they continuously communicate their state to each other. Using the information of each other's state, each unit determines the best control so as to maintain formation with respect to the other units. This scheme does not have a leader or master, instead the commanded formation defines the point in space where the formation centers; the units move around this point to maintain formation. The peer-to-peer scheme requires higher communications bandwidth and data processing than the other architectures. Since each of the units acts independently, it must be able to fully process all the information it needs for control;

further, it may have to work with the states of all the units in the system. All the units communicate their states to all the other units, therefore there must be enough bandwidth for all the units to transmit their states in real time. The peer-to-peer scheme would be reasonable for systems with a small number of units, but the communications and processing requirements make it impractical for large systems.

As FF systems get larger, having one single unit be the Leader or Master becomes impractical. A hierarchical structure, which combines instances of the architectures described above to control complex separated spacecraft systems, can provide a solution. For example, a 30 unit system may have three sub-systems. Each of these sub-systems has 10 units controlled via a Leader/Follower scheme. The Leaders of these sub-systems use a Peer-to-Peer configuration. By creating sub-structures, we allow the system to benefit as a whole from the Peer-to-Peer configuration for the Leaders; they are likely to maintain better formation between themselves. The sub-systems, in turn, have the lower processing and communications requirements of a Leader/Follower scheme.

The communications and processing requirements of a hierarchical structure depend on the sub-system architectures selected. Still, they do increase beyond the standard single architecture system, since the higher level units must be part of two different architectures. In the example, the three Leaders not only communicate their states to their followers, but also send and receive states between their Peers. Further, if a Leader fails, then one of the Followers must become a Leader with Peer-to-Peer capabilities if full redundancy is desired.

Figure 18 illustrates the operation of a real-time operating system and how the architecture selection affects the communication system. All satellites still maintain a real-time control interrupt which runs at a constant rate. A background process section transmits and receives non-critical data, as well as performs general housekeeping tasks. Recall that in a master/slave system the master performs all the control and computation, while the slave only provides sensing and actuation. These systems will require high bandwidth, high reliability, real-time communications. The master will have high computational requirements, while the slave will need minimal processing power. In a leader/follower system, the follower spacecraft will need to know the leader's state, but not necessarily at the constant rate of the real-time control; furthermore, communications can be simple high level commands. In this architecture both will require high computational power.

### **2.7.3 Results and Discussion**

Table 5 summarizes the processing and communication requirements, and presents a summary of the negative and positive aspects of each individual architecture. Hierarchical structures are not listed because their requirements depend on the selected sub-system architectures. The table shows the communications required for STS communications in terms of High, Medium, and Low bandwidths and processing requirements.

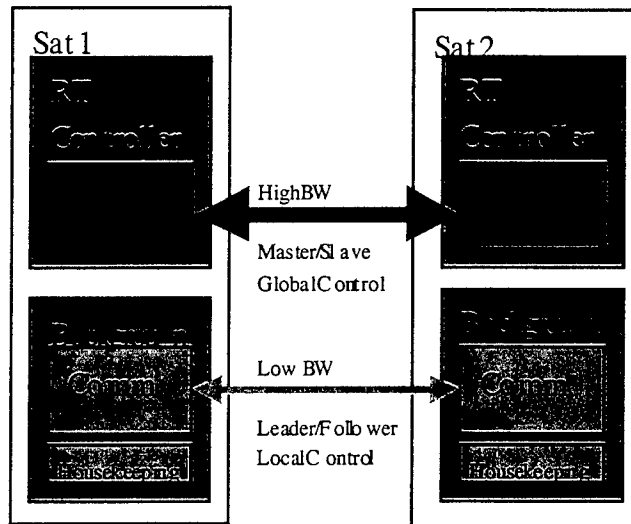


Figure 18. Software Architecture Effects on Communication Requirements

To motivate further study of formation flight algorithms, initial tests between independent units and a master/slave system were performed in the SSL SPHERES Formation Flight testbed (see §2.12). Under the selected architecture the master unit autonomously performs high-level commands received from the ground station and sends its state to the slave unit. The *smart* slave performs all the calculations necessary to follow the master by using the master state as its reference input.

Figure 19 presents the results of the independent units tests and the master/slave tests. Table 6 presents the numerical results, which indicate the total area between the curves of the commanded slew and the actual slew presented in Figure 19. The results demonstrate the ability of formation flight algorithms to obtain similar or better performance than independent slews. For this simple example, the two units had good quality gyroscopes that provided enough accuracy for the independent slew to be performed with little error. Yet, in the presence of disturbances, the independent units could not maintain formation. In the case of the master/slave system, the slew performed under the independent units because the slow rate of communications, at 10Hz, affected the controller performance. Yet, in disturbances, the units were able to maintain formation and produce a total error well below that of the independent units.

#### 2.7.4 Conclusions and Recommendations

The ability to overcome disturbances to members of a formation is critical to many of the programs that utilize separated spacecraft. In many cases the formation must be kept relative to each other, like in the case of observatories that use multiple apertures. The results encourage further demonstrations of formation flight algorithms with higher communication rates, better control theory, and using smarter algorithms such as the leader/follower or peer-to-peer. Formation flight spacecraft can maintain a better formation than independent units, and given the necessary bandwidth, should be able to perform coordinated maneuvers with the same accuracy.

Table 5. Summary of Formation Flight Architectures Requirements

Architecture	Prim ary Unit		Second Unit		Total System		Pros	Cons
	C	P	C	P	C	P		
Independent	L	M	-	-	L	M	<ul style="list-style-type: none"> <li>• Simplicity</li> </ul>	<ul style="list-style-type: none"> <li>• lack of redundancy</li> <li>• not enough accuracy</li> </ul>
Master/Slave (dumb)	H	H	H	L	H	M	<ul style="list-style-type: none"> <li>• simplicity</li> <li>• provides interconnection of units</li> </ul>	<ul style="list-style-type: none"> <li>• depends on highly reliable and fast communications</li> </ul>
Master/Slave (smart)	M	M	M	M	M	M	<ul style="list-style-type: none"> <li>• maintains some simplicity</li> <li>• separates processing needs</li> <li>• lower communications requirements</li> </ul>	<ul style="list-style-type: none"> <li>• slave is still blind to other units</li> <li>• not enough redundancy in system</li> </ul>
Leader/Follower	H	M	L	M	M	M	<ul style="list-style-type: none"> <li>• adds redundancy to system</li> <li>• followers are able to save power by processing state of leader</li> </ul>	<ul style="list-style-type: none"> <li>• higher processing requirements</li> </ul>
Peer-to-peer	H	M	-	-	H	M	<ul style="list-style-type: none"> <li>• highly redundant system</li> <li>• expected to have best accuracy</li> </ul>	<ul style="list-style-type: none"> <li>• high communications and processing requirements</li> </ul>

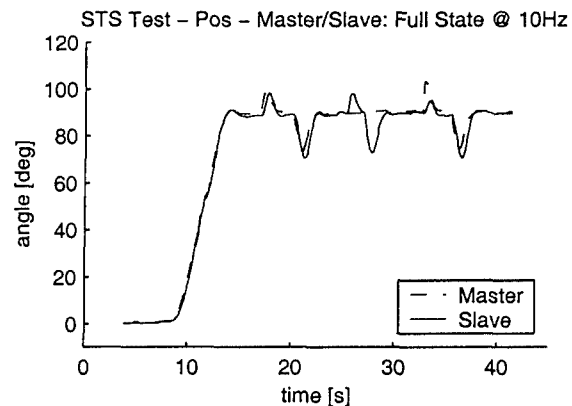


Figure 19. Formation Flight Experimental Results – 90° Slew Maneuver

**Table 6. Total Error (area between the curves) of Formation Flight Slew**

<b>Error During:</b>	<b>Slew</b>	<b>Disturbance</b>	<b>Total</b>
<b>Independent</b>	100	1,907	2,007
<b>Master/Slave</b>	180	1,153	1,333

## **2.8 Evolutionary Growth of Mission Capability**

### **2.8.1 Motivation**

At first glance, the advent of nano-satellites and the desire for ever finer resolution apertures are at odds with each other. Nano-satellites are small, while finer angular resolution requires larger apertures. However, sparse apertures composed of distributed satellites flown in formation can remedy this conflict by creating two complimentary types of apertures using principles of interferometry. The first type of aperture is the small, individual antenna deployed on each nano-satellite. This aperture determines the field of view of the system, which varies inversely to its diameter. The second type of aperture is that synthesized by the coherent integration of the signals measured by each of the smaller apertures in the satellite cluster. This second type determines angular resolution, which varies inversely with the dimension of the cluster.

This de-coupling of angular resolution and individual aperture size provides other benefits. If, for instance, 1) a mission requires a low cost demonstrator prior to commitment to an operational system, 2) full mission funding is unavailable in a particular year, or 3) system requirements are expected to grow over time, Distributed Satellite Sparse Apertures allow the mission to undergo a staged deployment. The first launch is the technology demonstrator. Once proven to work on orbit, additional satellites are launched and integrated into the cluster to increase capability on an as-needed, as-afforded basis. This paper presents the cost-benefits of such a scenario with specific focus on NASA's Soil Moisture Mission.

### **2.8.2 Approach**

A sparse aperture array is a pattern of apertures that serve the purpose of a single, much larger aperture. The fundamental benefit is that the sparse aperture array can have considerably lower mass and cost compared to the single, larger aperture. Since the array is sparse, each aperture only fills a small fraction of the area that would be filled by the single, larger aperture. This makes it considerably less massive and costly to build and launch. In addition, its supporting spacecraft (S/C) bus is proportionally smaller due to lower power needs, lower inertia to point and control, smaller deployment mechanisms, etc. When the mass and cost is added over all the S/C in the array, it is still less massive and costly. In addition, the DSSA array also benefits from learning curve savings in the production of multiple, identical S/C. If the deployment is staged over time, where some S/C are being manufactured while others are operating in orbit, there is

increasing confidence in the design being manufactured. If problems are revealed in the S/C operating in orbit, the production can be stopped or the design can be modified, thereby reducing the overall risk to the program. As S/C fail or become obsolete due to technological advances, they can be removed from the array and replaced with the upgraded S/C. The net effect is that the resources that support the development and operation of the mission are allocated in a fashion that best accommodates production savings as well as mitigation of risk.

While ground resolution is achieved through appropriate separation of the S/C, there are several sacrifices that one must make in order to reap these benefits. The first is sensitivity, which improves with collecting area. The DSSA array has considerably less collecting area and therefore sensitivity or signal to noise ratio (SNR). The second is ambiguity or uv-coverage. The system's uv-coverage determines how much of the energy measured by the system actually arrived along the line of sight of the instrument. Lower uv-coverage means that the system has higher sidelobes and ambiguity. This increases the probability that off-axis signals can be misinterpreted as having arrived from the ground location on which the line-of-sight has been steered.

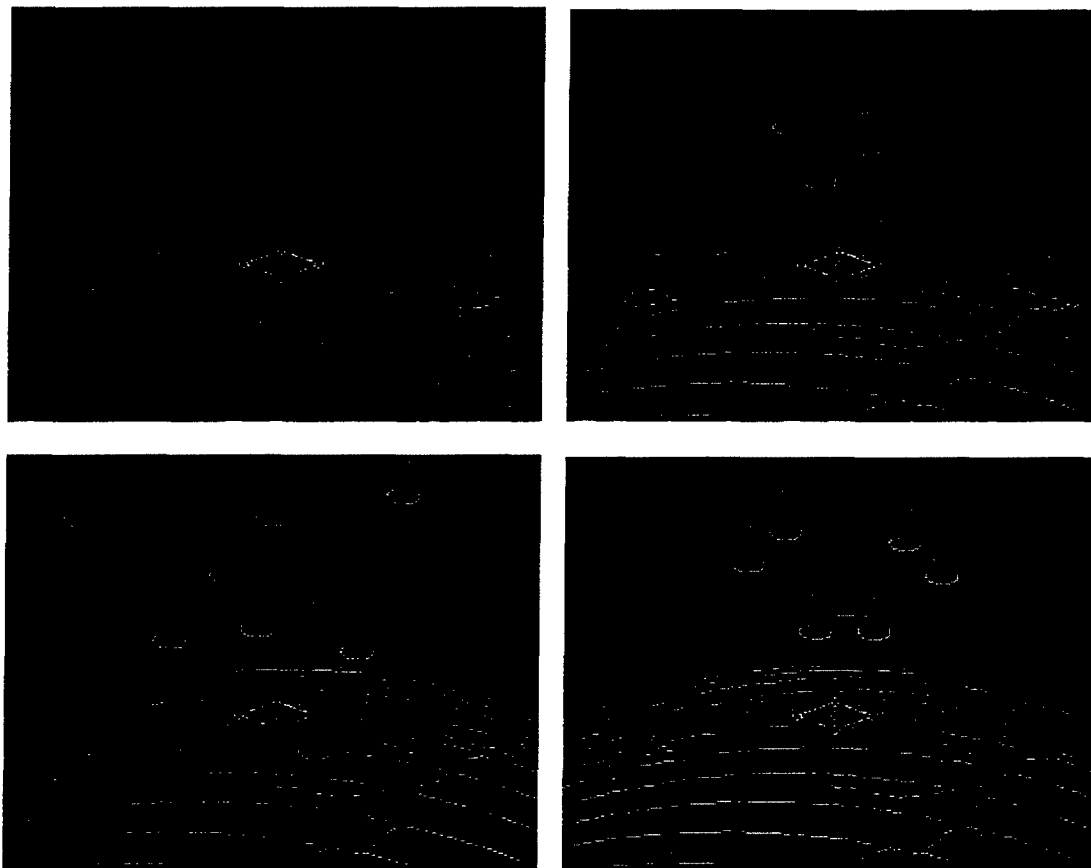


Figure 20. Concept for deploying aperture in a staged manner

The four images in Figure 20 show a candidate array at various times throughout its deployment. The upper left image is the single spacecraft demonstration associated with the EX-4 mission. Once confidence in the design is achieved, two more spacecraft are launched and formation



flown with the first (upper right). As funds become available and space-based experimental soil moisture science advances with the help of this system, three more spacecraft can be launched and integrated into the array (lower left). Due to aperture physics, the array may need to be reconfigured. The lower right image shows what an array might look like that provides the requisite 1 km ground resolution.

### 2.8.3 Results and Discussion

Figure 21a shows how fill factor decreases as the number of S/C increases. Figure 21b shows how the ratio of the DSSA Golay cost to monolith cost decreases as the number of apertures (S/C) in the array increases. Notice that the nine 8.3m diameter apertures needed to achieve 0.9 km resolution cost only 1.5% of the equivalent resolution monolith.

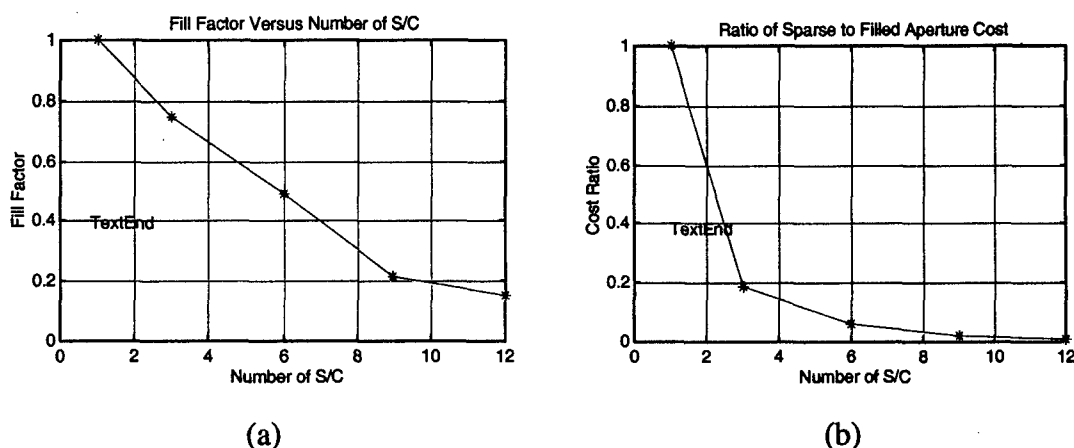


Figure 21. Fill factor and cost ratio versus number of spacecraft

In addition to Fill Factor, staged deployment is also a key to the success of DSSA Arrays. In the staged deployment scenario, the EX-4 mission is viewed as simply the initial launch of the operational mission. Once the aperture (S/C) design has been proven to be successful on orbit, manufacturing proceeds on the remainder of the S/C. As the array is augmented with subsequent launches, soil moisture scientists receive progressively finer resolution data, the engineers increase their confidence in the design (or implement design modifications to accommodate problems seen on orbit), and savings are realized through production learning curve effects.

A number of technical hurdles must be addressed for DSSA arrays to become feasible. Full u-v coverage requires the closest S/C to have their closest edges separated by one aperture diameter. This increases the probability of collision and plume impingement. Fortunately, perturbations caused by differential  $J_2$  become smaller as separations become smaller [8]. Control options include micro-propulsion, tethers, electromagnetic wands, orbital dynamics, and rendezvous and docking.

Rendezvous and docking could be accomplished using deployable magnetic wands, which are passive or active and would mate with equivalent wands on other S/C. Wands have bending stiffness (unlike tethers) to ease deployment and release dynamics. The Golay's central core could consist of several (e.g., 3) S/C docked in a triangular geometry with additional apertures as

formation flown outriggers. If a S/C fails, it can be released and replaced with a functioning S/C. The EM field could be varied by counter rotating permanent magnets or by varying power.

Alternatively, non-contacting extendable electromagnetic wands could be used. S/C counteract differential gravitational perturbations by exerting EM forces on neighboring S/C. This also has the advantage of not using valuable propellant. Differential  $J_2$  secular perturbation forces decrease linearly with array diameter while EM dipole forces decrease as the cube of the separation distance when separations are beyond the dipole length. Therefore, EM wands become ineffective beyond a certain separation. Extendable wands may allow EM dipole scale lengths to be beyond the spacecraft length, thereby increasing useable range. Outrigger S/C do not use their wands unless they are maneuvered to replace a failed S/C in the inner core. One could also use the wands to torque or force against Earth's magnetic field.

Tethers reduce the use of propellant, but increase dynamic and failure compensation complexity. Permanently attached tethers do not allow a failed S/C to be removed from the array. Attachable and detachable tethers allow reconfiguration of the array as well as replacement of failed S/C. Attachment of separated spacecraft has complex tether deployment dynamics (e.g., autonomous fly-fishing), however they could attach and detach while docked thereby requiring rendezvous and docking technologies to be developed.

Rather than use formation flight during operation, one could perform rendezvous and docking to build a structurally connected array over time. Elements are launched as secondary payloads at a fraction of the dedicated launch cost and rendezvous and dock with the array to increase its size. They would then cross-strap power and propulsion within the array. This architecture has the ability to compensate for failed elements. For example, if an element exhausts fuel, it could be moved to the interior of the array where no propulsion is required. If an aperture fails, it can be removed from the array or used solely for power and propulsion. If an element fails completely, it can be removed from the array.

As these arrays grow, there is a need to expand the navigational and metrology web for the array. Fixed, directional transmitters and receivers will be hard pressed to accommodate the addition of satellites above the number originally envisioned. A more distributed network that can accommodate any number of elements would be preferred. Missions that operate within the GPS constellation would have this capability.

Another challenge is low areal density radiometers. The mass and cost of radiometers drive the cost of the system. Therefore, lower cost radiometers would allow fewer S/C with larger apertures to be launched, thereby reducing operational complexity.

Further challenges include autonomous close proximity formation flight, rendezvous, collision avoidance, docking, alignment, cross-strapping, and reconfiguration. Autonomous management of distributed resources is essential to cost-effective operations and include concatenated array control, fuel balancing, fault detection, distributed consensus, and recovery. Clearly, distributed architectures provide more redundancy but also degrade faster. Optimization of productivity by optimizing reliability is an important aspect of making DSSA arrays more cost-effective. Cost modeling of operations and reliability would allow more comprehensive trades to be conducted.

## **2.8.4 Conclusions and Recommendations**

Distributed Satellite Sparse Apertures (DSSAs) revolutionize mission evolution from experimental demonstration to operational readiness. Experimental demonstration essentially involves check-out of the first element in the array. Once proven on orbit, confidence exists to launch additional elements on an as-needed, as-afforded basis. Technology upgrades can be incorporated in additional elements and the arrays can be grown beyond their original capabilities. DSSAs also pose new and complex challenges. In addition to currently envisioned formation flight, close proximity formation flight, electromagnetic control, and rendezvous and docking may be needed. After rendezvous and docking, precision alignment, power and propulsion cross-strapping, and control reconfiguration become essential. Inter-satellite navigation and metrology that is expandable as the array grows and autonomous operations for fault detection and recovery, fuel balancing, docking, and control reconfiguration are needed.

## **2.9 Optimization Approach to the Launch Vehicle Selection Process for Satellite Constellations**

### **2.9.1 Introduction**

In the next ten years, over 1000 new satellites are scheduled to be launched into orbit to provide a wide variety of services for military, civilian, and commercial customers. To be successful in this evolving market, systems engineers will depend on a wide range of support tools to help reduce program costs and mitigate program risk. Launch vehicle selection and deployment strategies are an important and expensive issue for satellite system development. Selection of a sub-optimal launch scheme can significantly impact cost and schedule parameters of a satellite constellation program. Satellite developers currently must choose from several dozen launch vehicle models, with many new vehicles scheduled to enter service within the next decade. This sheer magnitude of launch options complicates the selection process of a suite of launch vehicles for a satellite constellation deployment strategy.

Beyond launch costs, it is imperative that satellite constellation developers pay close attention to vehicle reliabilities. Unlike air transportation, space launch involves considerable risks. Launch failures such as the 1998 loss of 12 Globalstar communications satellites on board a Zenit 2 vehicle can be financially disastrous. The Globalstar failure resulted in millions of dollars in lost revenue for the parent company as well as a one-year schedule slip for market entry. The potential introduction of reusable launch vehicles designed for high reliability and low per flight costs into the decision matrix will further complicate the launch vehicle selection process as the number of available options increases.

The primary objective of the Launch Vehicle Selection Tool (LST) is to provide satellite constellation developers with a method for determining the optimal launch deployment strategy. Given the characteristics of a particular satellite constellation (number of satellites, satellite mass, spacecraft dimensions, orbital geometry, etc.), the Launch Vehicle Selection Tool determines the optimal combination of launch vehicles for the program based on three

optimization parameters (ie. objective functions): 1) minimization of total launch costs, 2) minimization of program risk, or 3) minimization of combined program costs and risk.

### **2.9.2 Approach**

In the launch vehicle selection problem, an organization would like to deploy a constellation of  $N$  satellites. The organization must choose from  $n$  different vehicles to launch its satellites. Each launch vehicle has a unique capacity (number of satellites it can place into orbit), risk, and cost associated with it. The system engineer's goal is to select the subset of launch vehicles that can deploy all of the satellites in the constellation at the minimum cost and/or risk; while at the same time adhering to a set of satellite, orbital dynamics, political, and availability constraints.

First, a database detailing the properties of all current launch vehicles was created. Next, the characteristics of the satellites in the constellation to be deployed were entered into a second database. With this information, preprocessing calculations were executed to determine how many satellites each rocket can deliver to the desired orbit. The problem was then formulated as an integer program (Table 7) and solved. The final solution was analyzed to determine the appropriate launch vehicle selection strategy for the given distributed satellite system.

### **2.9.3 Results and Discussion**

Three separate case studies of three very different constellations were selected to demonstrate the versatility of the Launch Vehicle Selection Tool. Table 8 lists the characteristics of each of the three case study constellations. It should be stressed that the constellations in these three case studies are similar, but not identical to, the constellations on which they are based. Figure 22 plots the full constellation deployment total launch cost of the optimized launch vehicle deployment strategy for each of the three objective functions in each case study. Notice how the objective function alters the final launch vehicle selection strategy. Minimizing risk leads to a more expensive strategy than minimizing absolute launch cost.

**Table 7. Integer Programming Formulation of the Launch Vehicle Selection Problem**

Mathematical Formulation	Explanation
Objective Function	
$\text{Min } \sum c_i x_i$	Minimize Costs
Subject to	
$\sum C_i x_i \geq N$	Total Satellite Deployment Constraint
$\sum x_i \geq OP$	Orbital Dynamics Constraint
$\sum x_{ik} \leq Q_k$ for all $k$	Federal Law/Quotas/Sanctions Political Constraints
$\sum x_{ik} \geq M_k$ for all $k$	International Consortium Political Constraints
$x_i$ integer for all $i$	Integrality Constraints
$x_i \leq A_i$ for all $i$	Availability Constraints
$x_i \geq 0$ for all $i$	Non-Negativity Constraints

#### 2.9.4 Conclusions and Recommendations

Use of an optimization solver electronically linked to a launch vehicle database provides tremendous versatility to the solution of the launch vehicle selection problem. This is especially important when working in the dynamic space launch market. New launch vehicles with differing capabilities and costs can be introduced, failures can ground operational launch vehicles, or quotas and export license blocks can be placed on vehicles from different countries by Congress or the State Department. The Launch Vehicle Selection Tool presented in this paper can be used to quickly and effectively find a new, optimized launch vehicle selection strategy for the full deployment, replacement, or replenishment of the satellites within a constellation.

**Table 8. Characteristics of the Three Satellite Constellation Case Studies**

	Weather Constellation	Telephony Constellation	Broadband Constellation
Case Study #	1	2	3
Based On	NPOESS	Iridium	Teledesic
Ownership	U.S. Government	U.S. Company	Intl. Consortium
Total # Satellites	9	72	288
# Orbital Planes	3	6	12
# Sats. Per Plane	3	12	24
Satellite Mass	910 kg	690 kg	500 kg
Satellite Cost	\$75 M	\$25 M	\$15 M

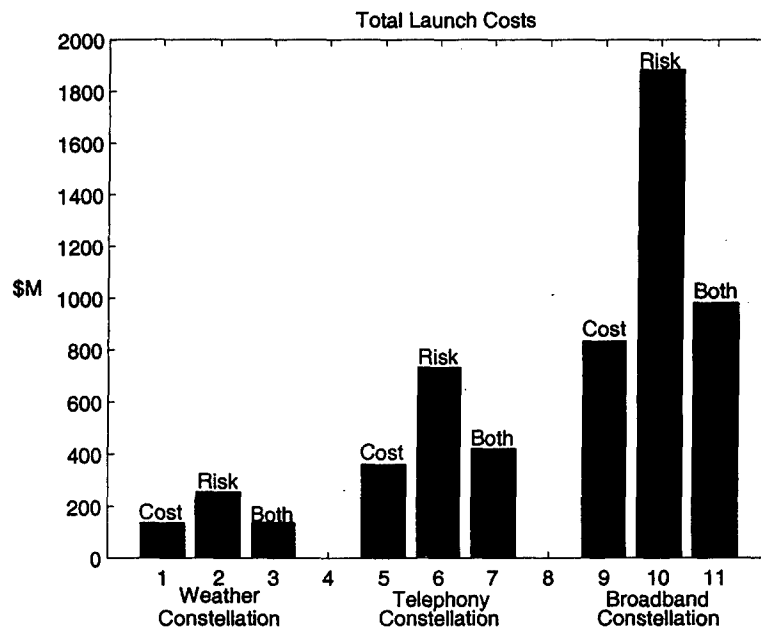


**Figure 22. Total Launch Costs For Different Objective Functions in the Three Case Studies**

## **2.10 A Systems Study on How to Dispose of Fleets of Small Satellites**

### **2.10.1 Introduction**

In more than four decades of launching spacecraft into orbit, many tons of man-made materials have been added to the natural debris already in orbit. As the human species relies more and more on our space infrastructure for communication, navigation, earth sensing, weather tracking, observation, and science, orbital debris will become increasingly threatening.

Orbital debris is a problem that will only increase in the magnitude with time unless something is done about it. A trend toward distributed constellations of satellites will magnify the proliferation of orbital debris unless satellites are designed with end of life disposal in mind.

To prevent a continued increase in the orbital debris population, three things must be done. First, spacecraft must be designed to minimize the inadvertent release of material into space. Secondly, all explosions of rocket bodies must be eliminated. Progress has been made in this area, but the complete elimination of on-orbit explosions by all space faring nations is necessary. Finally, spacecraft must be designed with a means for disposal at the conclusion of their useful lifetime.

### **2.10.2 Approach**

A systems study was conducted to determine the most mass-efficient method of achieving spacecraft disposal at the end of mission life. The focus of the study was on disposal by atmospheric reentry of constellations of small microsatellites in low earth orbit. Policy, tracking limitations, storage orbits, and natural orbit decay are important considerations with regards to spacecraft disposal. Various chemical and electrical propulsive technologies can be compared against tethers and ballistic coefficient altering techniques to determine the most mass-efficient method for disposal of spacecraft by atmospheric reentry within one year. It was determined that tethers and ballistic-coefficient altering methods are indeed the most efficient method of achieving atmospheric reentry of spacecraft within a certain range of altitude and mass. Tethers are the most mass-efficient method of spacecraft disposal for large satellites while decreasing the ballistic coefficient by deploying a balloon around the spacecraft or deploying a drag parachute is the most mass-efficient method for small spacecraft with a low initial altitude. The development of more advanced propulsion systems will be necessary to de-orbit small spacecraft at higher LEO initial altitudes.

### **2.10.3 Results and Discussion**

A method of disposal is considered to be the most efficient method if it can accomplish spacecraft disposal from LEO by atmospheric reentry within one year using the least amount of added mass to the spacecraft. A solar minimum condition ( $F_{10.7} = 65.8 \times 10^{-22} \text{ W m}^{-2} \text{ Hz}^{-1}$ ) was used for all calculations making the plots conservative for natural orbital decay, drag parachutes, and tethers. Figure 23 and Figure 24 detail the most efficient methods of disposal for average density and silicon satellites. The plots allow a mission designer to determine the most efficient disposal method based on the end-of-life altitude and mass of the spacecraft. The mass scale for

silicon satellites is smaller because it is believed the silicon satellites will enable a smaller class of satellites. It is believed that silicon satellites will be useful in the 100-kg class and smaller.

Figure 23 is a plot of the best disposal method for average density spacecraft. Average density spacecraft have been defined as those that have a density of  $79 \text{ kg/m}^3$ , the average density of spacecraft launched between the years of 1978-1984. The plot includes mission types where natural orbital decay, boosting to a storage orbit using thrusters or tethers, de-orbiting using thrusters or tethers, and deploying a drag parachute or balloon for disposal all make the most sense as a method of spacecraft disposal depending on the end-of-life altitude and mass of the spacecraft. Boosting to a storage orbit should be considered as a temporary solution and not a long-term method of spacecraft disposal. It is noted that with current tracking capabilities, average density spacecraft with dimensions less than 10 cm (approximately .1 kg) should not be deployed as they will be untrackable.

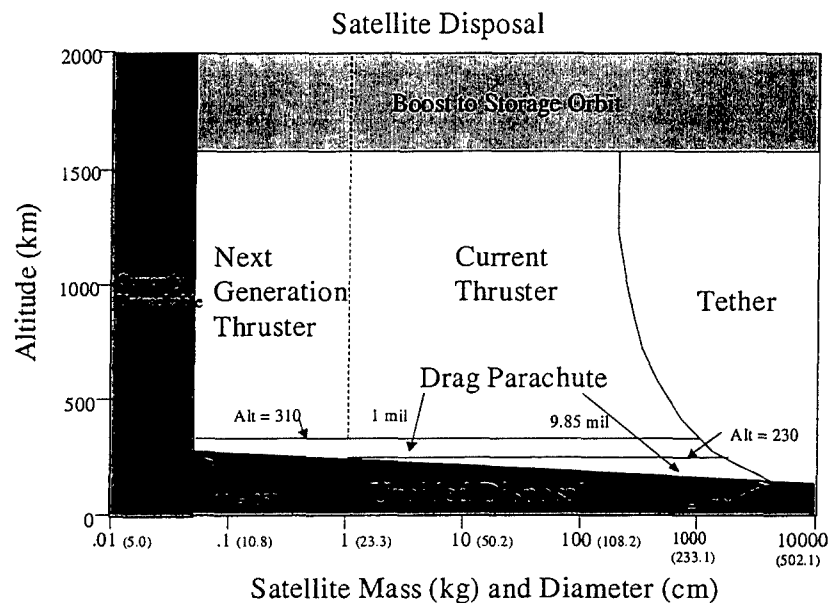


Figure 23. Most efficient disposal options for average density spacecraft

Like Meyer and Chao[9], this research discovered a range of missions where the use of a drag enhancement device such as a drag parachute or balloon proved to be the most mass-efficient method of disposal. But unlike Meyer and Chao, this work considered a time horizon of disposal of one year as opposed to 25 years. Plots in this work assume a solar minimum condition. With that assumption, the altitude below which a satellite will de-orbit within one year is determined to be 310 km. During solar maximum, a drag parachute is the most efficient method of disposal up to an altitude of approximately 350 km. It is also noted that at solar maximum the altitude from which a spacecraft will deorbit unaided by natural orbital decay within one year is approximately 40 km higher as well. A boundary is included between a drag parachute or balloon composed of material that is currently available and a minimum thickness drag parachute



or balloon composed of material completely resistant to atomic oxygen. In this research, the material considered for the drag parachute was the same as for a balloon.

Both chemical and electric propulsion systems are included in the “current thruster” and “next generation thruster” category. Decisions on what thrusting system to use should be based on the thrust and total mission  $\Delta V$  needed for the entire mission. A boundary is included between thrusters that are currently available and those that must be developed. The reason that current thrusters cannot be used efficiently on small microsatellites is that the propulsion system would make up a prohibitively large percentage of the spacecraft mass.

This research determined that the use of electromagnetic tethers is the most efficient method of disposal for all spacecraft with masses greater than approximately 1000 kg. Because such a large percentage of the weight associated with an electromagnetic tether system is the deployer, the added mass needed to scale a tether system to larger sizes is much less than the mass needed to add extra propellant for a thrusting system.

Determining the most mass-efficient disposal method was accomplished by modeling the various methods of disposal in a spreadsheet program. Mass must be added to spacecraft in the form of hardware, fuel, and necessary systems to accomplish de-orbit. These masses were computed based on assumptions detailed in previous chapters. After computing the added mass required to de-orbit a spacecraft within one year from LEO altitudes, the mass added was compared for the different methods as a percentage of the total spacecraft mass. The method that added the lowest percentage of additional weight to the spacecraft was considered to be the most efficient method. It is believed that plotting the results on a scale of end-of-life altitude versus mass would be most beneficial to a mission designer who can now determine the most mass-efficient method of disposal quickly.

Figure 24 is a plot of the best disposal method for satellites constructed exclusively of silicon. The mass scale in this plot is smaller than in Figure 23 because the silicon satellite concept enables smaller satellites and will most likely not be used in the construction of large spacecraft. The altitude scale is also smaller to show greater detail. For silicon satellites, like average density spacecraft, a satellite with dimensions less than 10 cm (or approximately 3 kg for silicon satellites) is untrackable and should not be deployed.

There is currently no efficient method for de-orbiting silicon satellites above approximately 310 km in altitude. Current propulsion systems would make up a disproportional percentage of the total mass of the spacecraft. Continued development of micropropulsion technology is necessary to provide a method of disposing silicon satellites at higher LEO altitudes.

#### **2.10.4 Results and Discussion**

A drag parachute or balloon is the most effective method of de-orbiting a silicon satellite below 310 km in altitude. Above approximately 310 km, the mass of the drag parachute system would total more than 10% of the total mass of the spacecraft. Drag parachutes can be used above 310 km, but the mass of the system will increase rapidly for de-orbit within one year. Figure 24 assumes a solar minimum condition. At solar maximum, the altitudes below which a drag parachute or natural orbital decay will de-orbit a spacecraft within one year can be raised

approximately 40 km. Meyer and Chao's work indicates that balloons are the most efficient method of disposal for spacecraft of this class up to an altitude of over 900 km. They come to that conclusion because they look at a 25-year time horizon that would include more than two complete solar cycles. Once again, a boundary is included in Figure 24 between a drag parachute composed of material currently available and a material that would be completely impervious to atomic oxygen erosion.

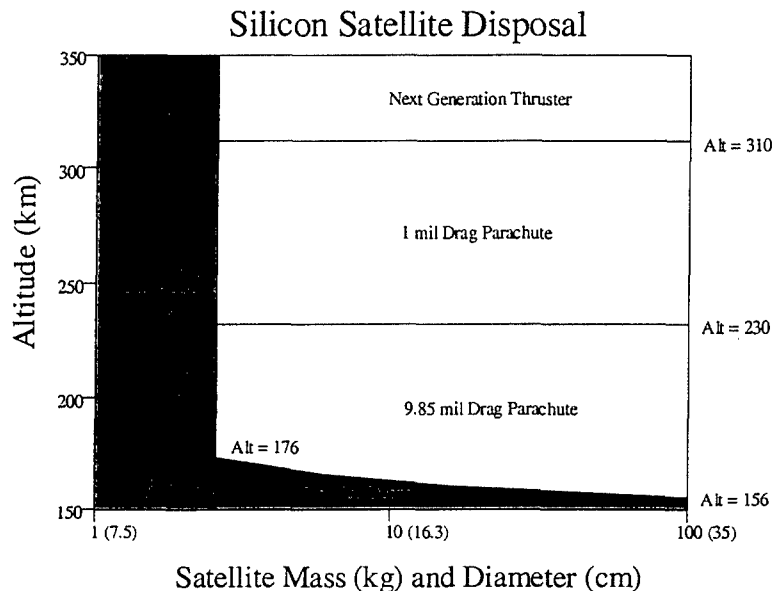


Figure 24. Most efficient disposal options for silicon satellites

## 2.11 Performance Analysis of a Space-Based GMTI Radar System

### 2.11.1 Introduction

In a departure from current space systems, a new design approach is being explored where clusters of micro-satellites flying in formation and operating cooperatively are used to perform the function of much larger, complex, and expensive single satellites. Each smaller satellite communicates with the others in the cluster and shares the processing, communications, payload, and mission functions. Thus, the cluster forms a "virtual" satellite. The TechSat 21 program was created to coordinate a wide variety of research efforts in this area of distributed satellite systems. Although there are many different application missions for satellite clusters, including surveillance, passive radiometry, terrain mapping, navigation, and communications, the initial reference mission for TechSat 21 is space-based ground moving target indication (GMTI) radar as it stresses many of the operational and hardware technologies required for a distributed satellite system. The GINA methodology has been applied during the conceptual design stage to the TechSat 21 mission in order to understand the global trade space of potential design architectures.

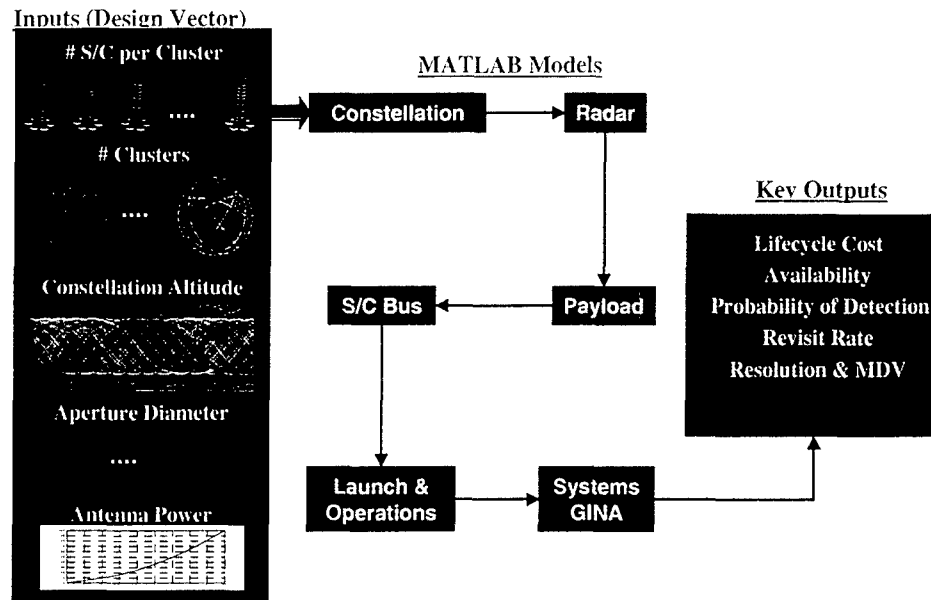


Figure 25. Top Level View of the TechSat 21 GINA Model

### 2.11.2 Approach

Figure 25 illustrates a top level view of the GINA model for the TechSat 21 mission. With the design vector inputs, the constellation module propagates the orbits of each satellite cluster to compute the coverage statistics of the particular constellation. Using these statistics in combination with the design vector inputs, the radar module calculates the expected performance of the radar system (probability of detection, availability, etc.). The payload module then sizes the radar transmit/receive antenna and computes its theoretical first unit cost. Once the payload has been sized, the spacecraft bus module sizes and costs the satellite bus required to support the payload. The launch and operations module then calculates the initial deployment cost, replenishment cost, and annual operations cost for supporting the constellation. Finally, the GINA systems module couples the reliability and lifecycle cost analyses. The outputs of the GINA TechSat 21 model include detailed subsystem specifications along with the GINA capability, performance, and cost metrics.

### 2.11.3 Results and Discussion

Figure 26 illustrates a sample exploration of the TechSat 21 trade space using the GINA model. Figure 26a plots the TechSat 21 system performance on the x-axis versus the system lifecycle cost on the y-axis of different TechSat 21 design architectures. The radial dashed lines represent iso-utility contours within the trade space, where utility is defined as the cost per unit probability of detection (ie. cost effectiveness) of the system. Figure 26b zooms in on the most cost effective region of the trade space shown in Figure 26a. The red asterisk represents a TechSat21 point design proposed by the Aerospace Corporation and the blue dots represent 1200 permutations (ie. 1200 different design vectors in Figure 26a) of the Aerospace Corporation baseline design. As one can see in Figure 26b, lifecycle cost tends to increase as performance improves. Notice that while the baseline design exhibits a high degree of performance approaching the theoretical limit, there appear to exist other design architectures within the system trade space that achieve similar good performance for a lower lifecycle cost.

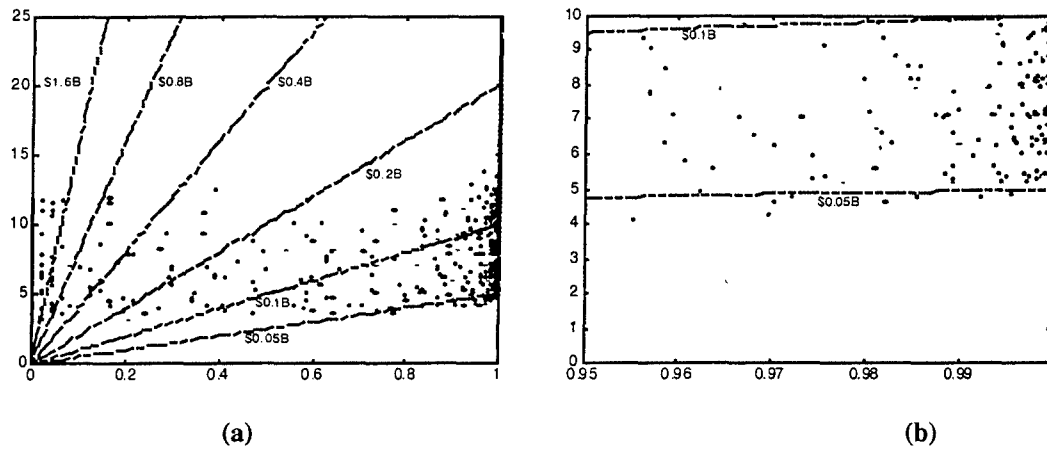


Figure 26. Aerospace Corporation Baseline Design Trade Space (a) and Trade Space Zoom-In (b)

#### 2.11.4 Conclusions and Recommendations

This simple two-dimensional (performance vs. cost) example illustrates how GINA may be used to find cost effective families of TechSat 21 mission architectures during the conceptual design stage. In more realistic design problems, the trade space may contain many more than two dimensions and several hundred thousand possible design architectures. In such cases, complete enumeration of the trade space is not possible. Special multi-objective search algorithms have been developed to search such TechSat 21 satellite constellation trade spaces (Figure 27) for the families of cost effective architectures.

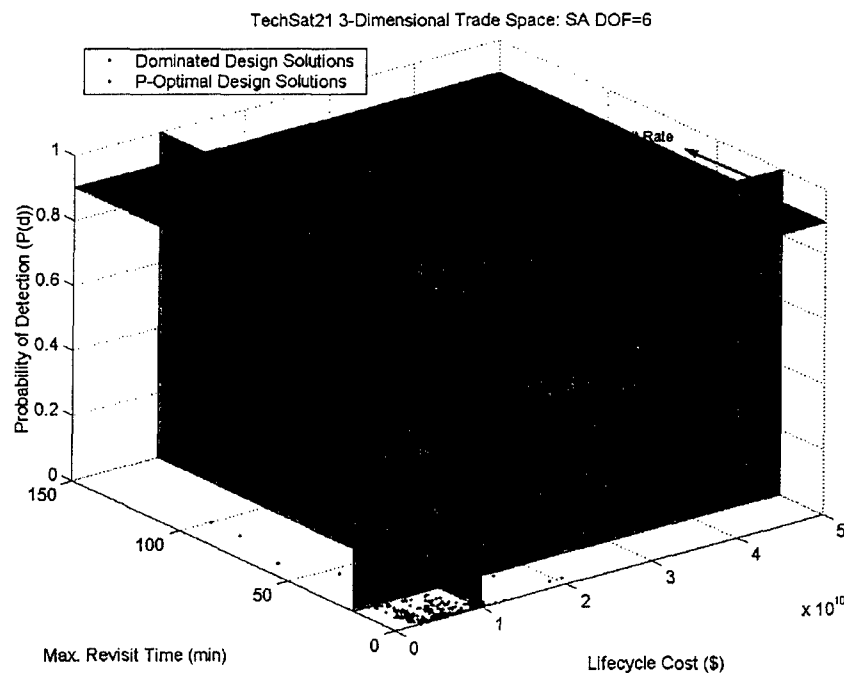


Figure 27. Multi-Dimensional Trade Space for TechSat21

## **2.12 SPHERES: A Testbed for Long Duration Satellite Formation Flight**

### **2.12.1 Introduction**

New space missions, under development at NASA and the Air Force, utilize Formation Flight technologies to take advantage of the improved angular resolution of separated spacecraft interferometers and distributed arrays. These advanced technologies, though, have not been proven, which presents a high risk for the success of the missions. The SPHERES Satellite Formation Flight Testbed provides these programs with a low-risk, low-cost environment to model, develop, debug, and optimize the control, metrology, and autonomy algorithms required for these missions. Utilizing the SPHERES testbed, these program can develop the control algorithms and implement them, obtaining hard data to demonstrate their validity. Further, due to the full 6 DOF operation of the SPHERES testbed and it use of technologies similar to those available in spacecraft, these algorithms can be easily upgraded to the final versions needed for space flight.

The SPHERES testbed consists of three independent re-programmable units that contain propulsion, communications, power, metrology, and software systems. A laptop computer works as the ground station to send high-level commands to the units and stores telemetry data from the units. Tests on one-g laboratory facilities and on NASA's KC-135 reduced gravity airplane have demonstrated the use of SPHERES to study and develop Formation Flight algorithms.

### **2.12.2 Methods, Assumptions, and Procedures**

Figure 28 shows the overall design of the SPHERES testbed. It shows the three independent free-floating units and the ground station/laptop. As shown, all units contain both satellite-to-satellite (STS) and satellite-to-ground (STG) communications. The metrology system transmitters are shown placed around the units. The transmitters are placed in known positions on the desired frame of reference; the units calculate their distance from each transmitter to determine their position within the frame. This section presents the design of the major SPHERES sub-systems: propulsion, power, avionics, communications, software, and metrology. The design requirements asked for functionality that closely resembles that of actual spacecraft, allowing the algorithms tested on the SPHERES testbed to be easily upgraded to flight software.

The propulsion system consists of a pressurized CO<sub>2</sub> system with micro-nozzles. The CO<sub>2</sub> is regulated to 70psi, which provides 0.25N of thrust from each of twelve thrusters. The thrusters are arranged around each SPHERES unit so as to provide full controllability. The major components are: tank, regulator, solenoids, and nozzles. Figure 29 shows the arrangement of these parts, chosen so as to ensure constant pressure among all the valves; note the addition of two 'reserve tanks' for this purpose. Testing of the SPHERES units has shown that the propellant lasts for approximately 10 minutes of normal operation.

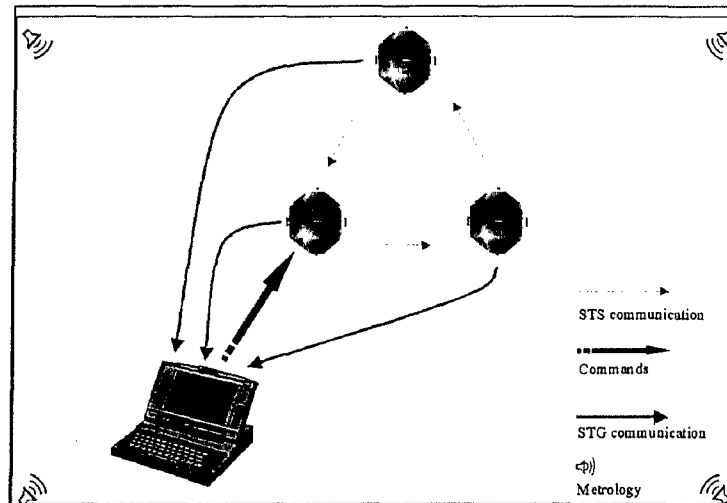


Figure 28. SPHERES Testbed Overview

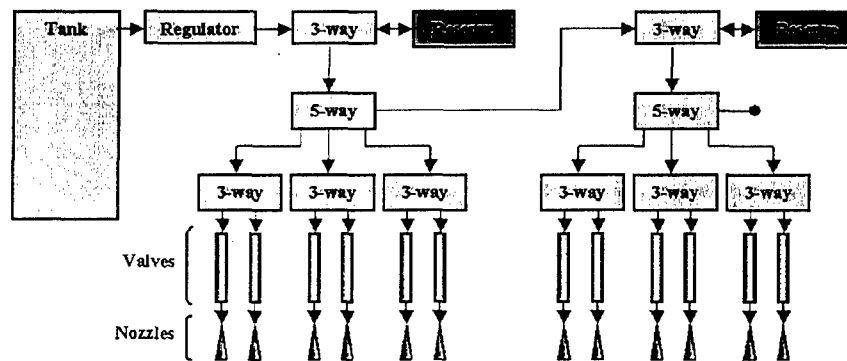


Figure 29. The SPHERES Propulsion Subsystem

The power sub-system provides electric power to all the other sub-systems via a electronics compatible with the KC135, Space Shuttle, and ISS. The voltage needs of the different sub-systems are 3.3V, 5V, 12V, and 24V. The total power requirement is approximately 6.6W. The system utilizes thirteen (13) AA alkaline batteries, which provide a total voltage of 19.5V. The demonstrated lifetime of the batteries, during actual operation in both a one-g laboratory environment and the KC-135, is approximately 90 minutes.

Two micro-processors are used in each SPHERES unit. A TIM DIO-40 board manufactured by DSP Systems Inc., based on the Texas Instruments C40 Digital Signal Processing (DSP) chip, was determined the best option for the main software processor. A Motorola 68K processor based board, Onset Technologies' Tattletale 8 (TT8), was selected to support the metrology functions. The decision to use two processors arose from the need for multiple DIO and analog lines in the same system and the need from the metrology system to support several multiple

level interrupts asynchronously with the rest of the software system. Table 9 lists the features of the selected microprocessors.

Each SPHERES unit uses two separate frequency communications channels with a data rate of 19.2kbps. One channel is used for satellite-to-satellite (STS) communications; the other channel enables satellite-to-ground (STG) communications. Both channels are bi-directional. Yet, the selected hardware is half-duplex, meaning that only one unit can transmit at a time. This requires the implementation of a communications protocol that ensures only one unit communicates at one time, but also that all units are allowed to communicate when necessary. The developed system implements a token ring network that uses packeted data. The token ring protocol ensures that only one unit transmits data at a time. Given the two communication channels, there are two token ring networks: one for the STS network and one for the STG network. The packet format includes the addition of a header with origin, destination, length, and packet type information, plus a tail that contains checksum information. This type of packet allows binary data to be transferred easily, and allows for error detection in the receiving end.

**Table 9. Micro-Processors of each SPHERES Unit**

<b>Feature</b>	<b>TIM DIO40</b>	<b>Tattletale Model 8</b>
Processor	TI TMS320C40	Motorola 68332
RAM	4 MB	1 MB
FLASH	512 KB	256KB
DIOs	32 I, 32 O, 32I/O	16
Analog Inputs	0	6
MHz	50	16
MIPS	25	4
MFLOPS	50	n/a
Mass	28g	90g
Power	3W	2W

Figure 30 presents the different components of the software architecture. The main components are the controller interrupt, software interrupt, and background processes. The other shown functions are parts of the software architecture that may be exchanged between the different sections of software in order to program the SPHERES testbed with a specific algorithm. The shown placement is an example of how the SPHERES testbed can work as independent units. The propulsion interrupt operates at 1KHz, the controller interrupt at 50Hz, and the background processes run freely. The controller interrupt is considered the main section of the software. This process determines the state of the unit, runs the control algorithm, and determines the necessary output. The propulsion interrupt provides the interface to the thrusters. By running at

1kHz it allows a minimum pulse width of 1ms (although the solenoids place a hardware restriction of 5 ms). The background processes are not time-dependent; they do not need to run at a specific rate. These processes run freely on the background, while neither of the interrupts is being processed.

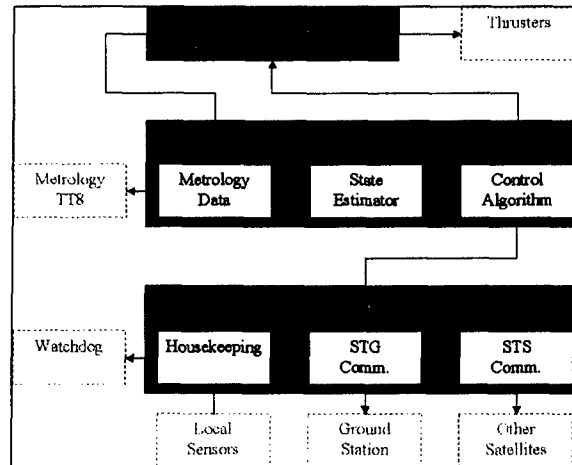


**Figure 30. Software Architecture**

The function of the metrology system is to determine the full state of the SPHERES units continuously. The full state includes determination of the linear position (for example, X, Y, Z coordinates) and angular attitude (for example, the rotation about the aforementioned axes). The full state of each unit is composed of the positions and angles, as well as their first order derivatives (velocities and rates); therefore the metrology system must determine both the positions as well as the rates of the SPHERES unit. The numerical requirements set forth to the metrology system are: position accuracy of 1 mm, attitude accuracy of 1°, and refresh rate of 50 Hz.

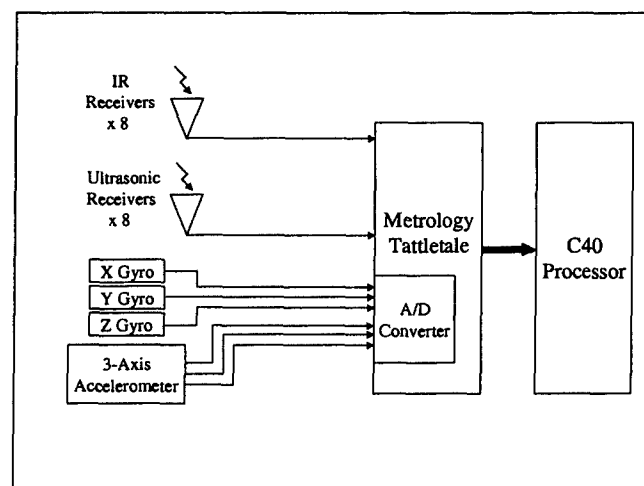


**Figure 31. The SPHERES Metrology System**



The metrology system utilizes two sub-systems to determine the state of the unit. An Inertial Measurement Unit (IMU) determines translation accelerations and rotation rates. Due to the drift of the IMU components, the information from this sensor must be updated. A ranging system based on infrared (IR) and ultrasound (US) signals is used to determine the position and attitude of the SPHERES with respect to an external reference frame. This measurement is used to update the IMU sensors. Figure 31 presents the block diagram of the metrology system.

### 2.12.3 Results and Discussion

One-g laboratory tests demonstrated the functionality of the SPHERES testbed. This demonstration included the ability to program a FF architecture using the SPHERES units, to perform the corresponding autonomous maneuvers, and to download telemetry data for subsequent analysis. The ability to program a FF architecture demonstrated the operation of the avionics and software systems. Performing autonomous maneuvers proves the functionality of the propulsion, power, and metrology systems. Downloading telemetry data, and performing FF maneuvers, demonstrates the functionality of the communications system. Results of these tests are presented in Section 2.7.

The goal of the KC-135 flights was to demonstrate the operability of the SPHERES testbed in a micro-gravity environment. This included the ability to propel itself in full 6-DOF, obtain metrology readings correctly, perform communications while rotating and translating in all directions, and demonstrate the ability to operate fully untethered for reasonable periods of time. The results of these tests proved full operation of the majority of the SPHERES systems, with a few upgrades under progress in the present. A limited set of master/slave architecture (see §2.7) tests were performed to show the use of SPHERES as a formation flight testbed in full 6DOF. Their main test kept the master attached to the KC-135 frame to prove the ability of the SPHERES units to keep up with the KC-135 motion.

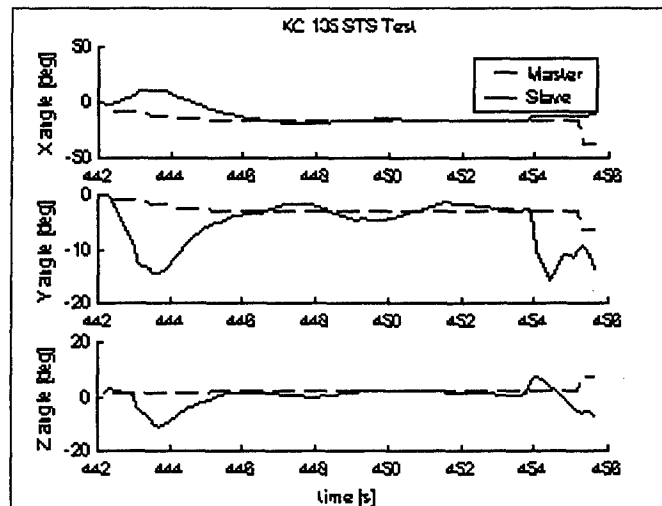


Figure 32. Master/Slave: Master Fixed to KC-135 Frame.

During the twelve seconds of micro-gravity operation the units are deployed (442-448), the Slave tracks the Master (446-454) while the KC-135 remains in a steady fall, and the units are then recaptured by a team member (454-456).

Figure 32 presents the results of the master/slave configuration when the master was attached to the KC-135 frame. The IMU measurements of the Master, therefore, present the sensed motion of the KC-135 by the SPHERES units during the micro-gravity portion of a parabola. During these test the master unit was aligned with the KC-135 frame in the following order: +X axis pointing towards the right wing (pitch), +Y axis pointing fore (roll), and +Z axis pointing towards the ceiling (yaw). Note the limited amount of micro-gravity time available (under fifteen seconds). This limited time during the tests is due to the initial deployment time of the SPHERES units and the imperfections in the KC-135 parabola due to turbulence and other external disturbances.

## **2.12.4 Conclusions and Recommendations**

The SPHERES project has been tested in two different settings: the one-g laboratory setup and the KC-135 reduced gravity airplane micro-gravity environment. The laboratory tests served to prove the overall functionality of the SPHERES testbed. The tests demonstrated operational propulsion, communications, software, power, and inertial metrology systems. Further work is being done to improve the global metrology system. Even in its early stages, the SPHERES testbed has provided insights into the use of Formation Flight algorithms. Therefore, the testbed will continue to be used to mature the different algorithms that will enable this technology.

## **2.13 Acoustic Imaging Testbed for Spacecraft Cluster Autonomy**

### **2.13.1 Introduction**

Sparse aperture systems replace a single large antenna with a number of carefully positioned smaller ones. This allows the system to function with the angular 'effectiveness' of a much larger system. By placing each aperture on a separately orbiting spacecraft, the system response can mimic that of a single antenna the size of the entire satellite cluster. Disproportional cost inflation and physical limitations of launch-vehicle fairings can then be avoided. Interferometry can be used in communications to create a high directional gain, in an astronomical interferometer to provide fine angular resolution, or in a radar system to maintain high probability of target detection.

The Acoustic Imaging Testbed (AIT) system employs hardware and software to create a functioning interferometer system [10]. As the name implies, the system operates using sound rather than electromagnetic waves. Sources are speakers, and sensors are microphones. This allows the testbed to provide a platform to examine common interferometry issues relating to systems and software in isolation from hardware challenges. The coordinated maneuvers of four mobile apertures are used to make observations and synthesize images of the sources. The operation of the AIT captures elements of both visible/IR and radio frequency interferometry. The spacecraft cluster concept is indicative of optical imaging interferometry, or cluster radar systems. Operating in the audio regime allows the source signals to be recorded and then processed off-line. Consequently the closest signal processing analogs are those systems using radio waves such as radar or radio astronomy. For technical simplicity, the type of processing

done with the AIT mimics astronomical imaging rather than the Doppler based detection of GMTI radar.

An interferometer achieves its excellent angular resolution through the measurement of the visibility function. A Michelson interferometer, such as the one shown in Figure 33a, consists of two sensing apertures separated by a vector displacement. This relative displacement vector is referred to as the baseline. A measurement taken at a particular baseline is equivalent to sampling a certain spatial frequency of the visual field. Interferometric imaging requires a number of visibility samples. Each measurement provides additional information about the brightness distribution and improves the quality of the image.

### 2.13.2 Approach

The AIT architecture maps the operational concept of a separated spacecraft interferometer (SSI) onto a simplified apparatus. Hardware provides the physical interaction and the medium for performing interferometry. The software establishes a consistent and simplified environment in which cluster automation can be developed. Finally, the 'intelligent' logic of the virtual spacecraft captures many of the high level decision-making problems faced by an operational system. Many functions must be accommodated in the architecture design: External users require a means of interacting with the AIT, logical spacecraft must be represented, and access to sensor and actuator hardware must be integrated.

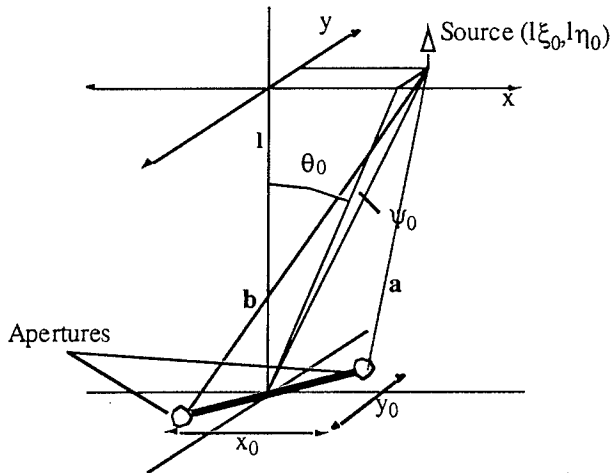
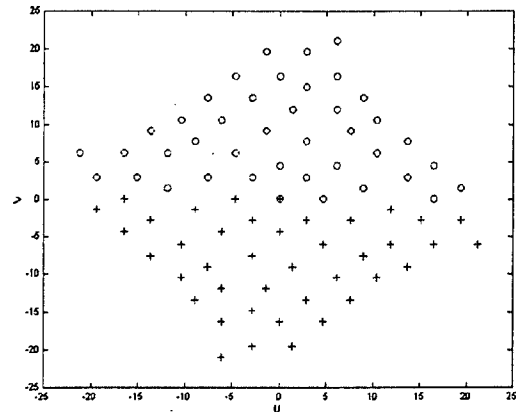


Figure 33. a) Interferometer Geometry



b) 40 Baseline Sampling Pattern

The hardware systems of the AIT encompass support computers, data acquisition, motion control, robotics, and other miscellaneous hardware. A distinction can be made between primary hardware and support hardware. Primary components are those subsystems that are most directly traceable to an SSI function. Support hardware, in contrast, are those pieces of equipment designed to facilitate the operation of the representative systems. The largest component in the AIT system is the anechoic chamber. Mounted within is the array of speakers that act as the imaging targets. Four robotic arms, each equipped with a tip-mounted microphone, complete the set of primary hardware. Data acquisition and motion control electronics constitute the secondary systems

If the AIT hardware is to provide the physical representation of the interferometry process, the software must provide a mapping between the actual hardware and the environment. There are two primary tasks that must be accomplished; develop 'intelligent' spacecraft logic, and more fundamentally, to provide the environment that allows these agents to interact. Some practical concessions were necessary during design. For cost and simplicity reasons, the testbed does not possess four separate sets of sensing and actuation hardware. The cluster shares a single sensor interface and a single actuator interface. Although this creates a slight compromise in the AIT's accuracy of representation, corrections can be made through careful engineering of the software environment. Thus, each of the spacecraft agents perceives that they have their own dedicated sensing apparatus.

Each time the apertures move, their relative, pair-wise spacing creates interferometer baselines. Each pair of measurements must be *correlated* to yield the visibility measurement. This correlation process represents an enormous reduction in the volume of data, so performing this operation within the cluster, rather than on the ground, translates to a much less demanding requirement on the communications system. However, it is essential that the nodes hold this information before the computation can start. Some mechanism to share the data must also be provided. While a central processing spacecraft for the entire cluster represents a possible implementation, most schemes considered to date have involved identical spacecraft. Thus, each spacecraft must operate as an individual processing unit and perform a fraction of the aggregate processing.

### 2.13.3 Results and Discussion

Imaging using the AIT is rapid and requires little intervention from the user during nominal operations. Maneuver sequences of various lengths were evaluated for both single and multiple target configurations. Some example images are provided in Figure 34 and Figure 35. Post-processing techniques based on deconvolution [11] were introduced as a means of image enhancement. Very encouraging results were observed using the CLEAN algorithm (Figure 35b). The resulting images suggest that in situations where detection is more important than high resolution imaging, good results can be obtained with only a small number of visibility samples. Although the implicit assumptions of the CLEAN algorithm, limit its use to astronomical observations, other techniques are applicable to radar systems [12].

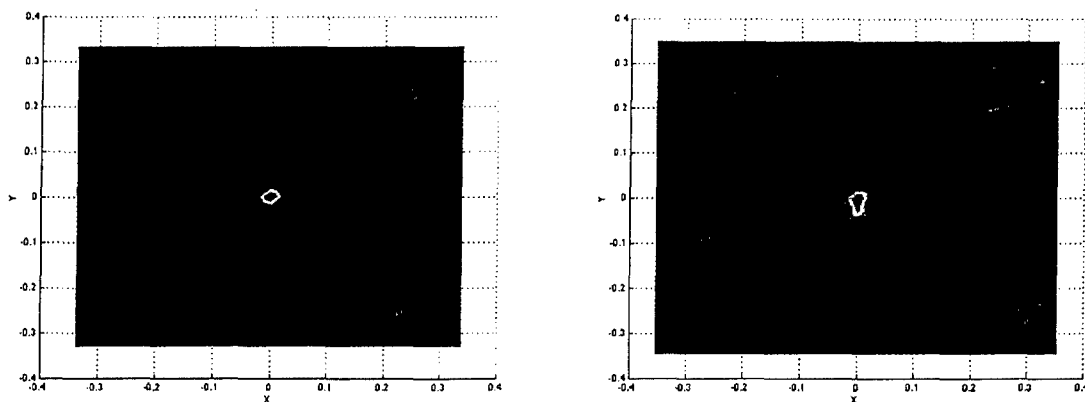
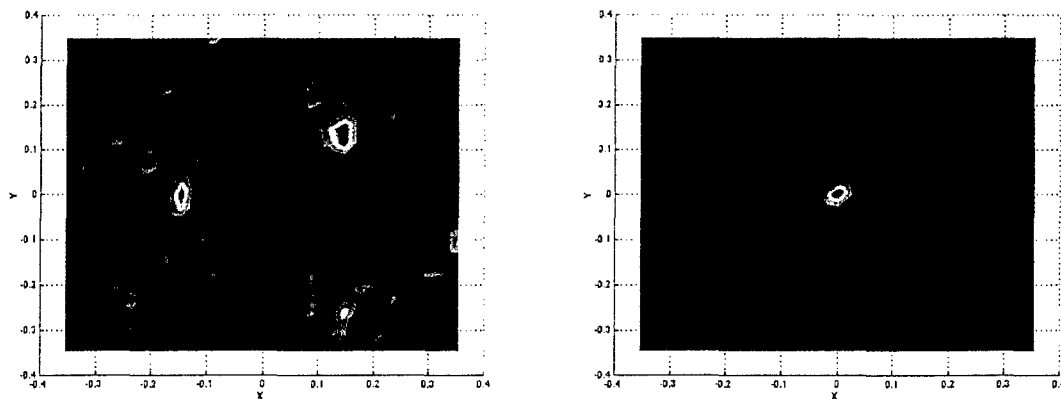


Figure 34. a) 40 Baseline, Ideal Response

b) 40 Baseline, Meas. Response



**Figure 35. a) 40 Baseline, 2 Sources**

**b) Processed 40 Baseline Image (1 source)**

End-effector positioning accuracy caused by hardware limitations was found to be significant error source. Sadly, the degradation of image quality caused by mechanical difficulty prevented advanced validation of the optimized array configurations. While validated at the qualitative level, quantitative performance assessment was not possible. Permanent improvement would have required redesign of the robotic hardware.

## 2.13.4 Conclusions

The successful layering of hardware and software provided a multi-agent simulation environment capable of representing essential cluster behaviors such as communication and coordination. Subsequent addition of a dynamic simulation environment and a more complex function enable more complete understanding of the factors affecting autonomous implementations of sparse aperture using spacecraft clusters.

The AIT digital signal processing is most directly analogous to astronomical radio systems [13]. An astronomical radio-frequency cluster is a difficult concept to envision since the spacings between elements would have to be huge. Very Long Baseline Interferometry uses a combination of ground and space observations. A 'cluster' solely devoted to radio interferometry would have to be of similar size to add greater functionality. At such sizes, it would resemble a large constellation rather than a closely-knit cluster. The capacity for coordinated actions would be greatly reduced. On the other hand, localized clusters would be acceptable in a ground looking radar system. The specific processing methods are different but the distribution and autonomy issues are similar. With some adjustment in the signal processing algorithms, such a system would be very well represented by AIT operation.

## 2.14 Generalized Flight Operations Processing Simulator

### 2.14.1 Introduction

The *Generalized FLight Operations Processing Simulator (GFLOPS)* is designed to provide an environment for high-fidelity, real-time simulation of distributed satellite systems (DSS). In *New World Vistas*, distributed satellite systems were outlined as one of the key future

technologies for the US Air Force.[14] Not surprisingly for a revolutionary technology, DSS brings myriad new challenges that must be overcome. One of these is formation flying, or maintaining precise relative position between members of the satellite cluster. Since this new requirement does not exist for traditional monolithic spacecraft, extensive simulation is needed to verify control algorithms. For interferometric imaging missions, such as space-based radar, there arises the need to efficiently process images from each of the satellites in the cluster at a given rate. This introduces the question of how to best distribute the processing among the satellites. Although a solution could be arrived at on paper, one also needs to verify the choice and test its performance through simulation.

Even more ambitious is the leveraging of techniques of artificial intelligence to achieve a level of spacecraft autonomy. For several decades, researchers in *artificial intelligence (AI)* and autonomy have recognized that certain areas of space engineering can benefit considerably from 'smarter', more capable software. This is especially true for large constellations, where the number of satellites makes traditional ground control prohibitively complex and expensive. However, concerns about reliability have limited the applications of autonomy technology to situations in which traditional methods have proved inadequate. Usually this meant critical phases of interplanetary missions where propagation delays prevented traditional ground-based commanding. But if we want a spacecraft to achieve the capabilities of health and status monitoring, plan generation and robust execution, autonomy must be applied in a more general sense to the mission. Clearly, this would require thorough pre-flight simulation and testing, an endeavor for which GFLOPS is ideally suited. By serving as a simulation environment for distributed satellite systems, and as a proving ground for new ideas and technologies, GFLOPS can help bridge the gap between current satellite technology and the future needs of the Air Force.

Another motivation for GFLOPS is to provide a set of design guidelines and tools to improve the engineering of spacecraft flight software (FSW) through its entire life cycle, resulting in greater speed, reliability and innovation in FSW. This set of guidelines and tools is termed the GFLOPS Rapid Real-Time Development Environment (GRRDE).

### **2.14.2 Methods, Assumptions and Procedures**

As one might expect for a DSS simulation, the GFLOPS framework is inherently distributed. A schematic representation of the test-bed hardware is given in Figure 36. The distributed simulation framework results in separation of the flight software and simulation software, reducing the possibility of FSW logic being tied to the simulator instead of reality. It also allows for the FSW running on the embedded processors to be as close as possible to the actual FSW that would fly on a satellite.

Eight PowerPC-based computers represent a modern family of processors currently being investigated for space applications. Simulation tasks and user interface are the responsibility of several common PCs. These support tasks are partitioned into three categories:

- 1) Payload: All simulation tasks related to the primary mission purpose

- 2) Orbit/Environment: Environmental effects, orbit/attitude propagation as well as spacecraft subsystem simulation
- 3) Ground Terminal: Acts as the user's access to the system. Capabilities similar to operator or end user's workstation.

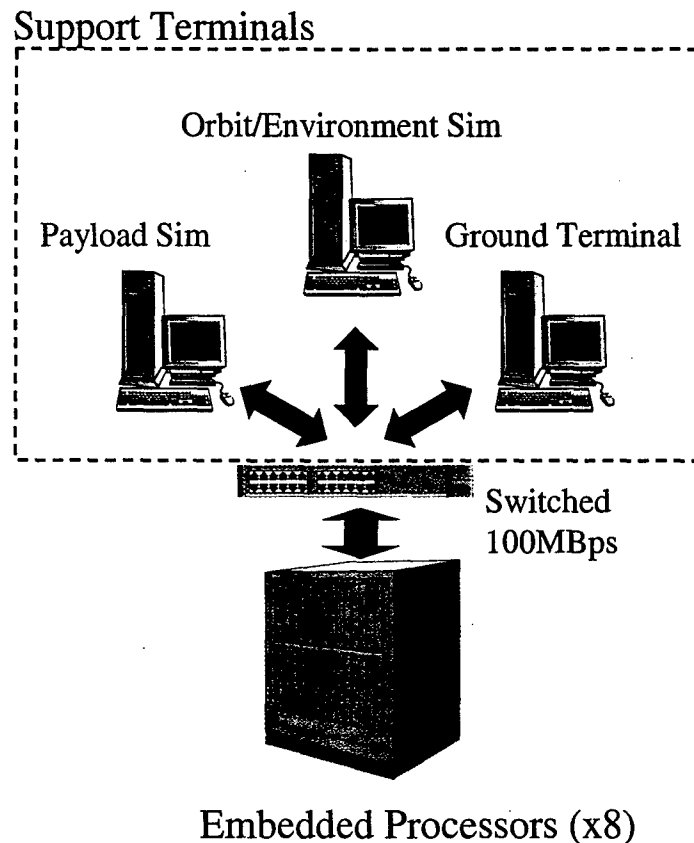


Figure 36. Schematic of GFLOPS Testbed Hardware

A Fast-Ethernet LAN provides interconnection between components. The capacity of Ethernet is reasonably representative of both space to ground communication and inter-satellite links. It does not, however, provide a good mechanism for representing transmission errors, antenna tracking or latency. A summary of the hardware selection is given in Table 10 at the end of this section.

GRRDE is designed to operate with the OSE operating system provided by ENEA Systems. OSE is a modern real-time OS that supports many features that make it particularly appealing for use in distributed systems. The process model is based upon priority assignments and preemption. Prioritized processes are designed to handle the bulk of system load, but other process types are also supported (i.e. timer/HW interrupts, background). Flexible memory protection is offered and the designer can group related processes into common address spaces. In OSE, Inter-Process Communication (IPC) is achieved through message passing. The IPC operates transparently across memory protection boundaries and through network links. The operating system supports

the capacity to load executable code at runtime. This useful feature is a boon to simulation debugging in which the correction of small errors does not require rebuilding the entire system.

**Table 10. GFLOPS Hardware List**

<b>Embedded Processors</b>	
Manufacturer	Force Computer
Model	PowerCore-6750
Processor	PPC-750
Speed	400 MHz
Memory	256 MB
<b>Support PCs</b>	
Processor	Pentium III
Speed	600 MHz
Memory	384+ MB
<b>LAN</b>	
Switch Type	3Com SuperStack 100BaseT

The philosophy of GRRDE is to take an aggressive approach to adopting contemporary software engineering tools, while retaining credibility with the spacecraft software community. Thus, the choice of programming languages must balance traditional real-time concerns of determinism, speed and space efficiency with more modern interests in readability, extensibility and expressiveness. To achieve these goals Embedded C++ (EC++) has been chosen as the standard for GRRDE flight software development. EC++ is a subset of modern C++ that includes many of the important features of Object-Oriented Programming while dropping those features that are not suitable for embedded applications. The interested reader is encouraged to refer to the official reference for further information.[15]

Modular software design is a central theme of the project. This includes both the use of the complementary notions of *Object-Oriented Design* and *Object-Oriented Programming*, as well as the decomposition of software into independent modules based on subsystem function. This promotes code reuse and allows for seamless upgrading of the simulation modules. From the design process, specifications are developed for each functional module. The specification process describes the abstract function of each module (including timing information), its inputs, its outputs, and lastly any external dependencies. A central tenet of the GRRDE design process is to think of these features in terms of *state information* (or simply *state*). One of the primary run-time services provided by GRRDE is a generic mechanism for state transport. Known as the GRRDE State Contract Architecture (GSCA), it allows for flexible configuration of information pathways. These features de-couple the process of creating state information from the act of distributing it. Thus the logic of a module can be written without reference to the precise origin or destination of its inputs and outputs.

### **2.14.3 Results and Discussion**

The GFLOPS simulator has been tested with several simulations that have demonstrated simple attitude control and formation flying capability. These have verified the usefulness of the



GRRDE toolset and the simulation framework. Realistic gravitational disturbances as well as sun/moon influences are used to propagate satellite trajectories. GRRDE permits efficient code development and enables easy reconfiguration of simulations by swapping one module for another. MATLAB real-time code generation facilities have been customized to automatically generate OSE modules. This creates all of the initialization, synchronization and state transport code. Currently, integration of the Spacecraft Command Language (SCL), a real-time scripting language and real-time inference engine, is being investigated. Because SCL has been employed on several real satellite missions, the ability to use SCL with GFLOPS would greatly enhance the usefulness of GFLOPS as a FSW development environment and simulation tool. A thorough simulation of the USAF TechSat21 distributed satellite system is also being developed. This simulation will focus on ground moving target indication (GMTI) and will investigate possible image processing architectures for the system, as well as the integration of autonomous capability. Some of the autonomy tools that will be implemented on GFLOPS are a model-based mode estimation system known as MiniME and a scheduler/plan runner.

#### **2.14.4 Conclusions and Recommendations**

GRRDE and GFLOPS have demonstrated excellent capabilities as a tool for developing space flight software and an environment for simulating distributed satellite systems. The GRRDE approach to software design has proven to be very beneficial to flight software development in our simulations, minimizing development and debugging time. The study has also demonstrated the suitability of OSE as a real-time distributed operating system and of embedded C++ as a programming language for FSW. The ongoing simulation of the TechSat21 system will provide an invaluable analysis of this mission, allowing for investigation of possible processing architectures, parameter optimization and autonomy integration.

### 3.0 CONCLUSIONS

The DSS program has both taken a broad view of the issues associated with the distribution of satellite resources, as well as looked in great detail at several of the leading technologies which support this practice.

In capturing the essential physics of all mission aspects, the GINA systems engineering methodology enables a comprehensive exploration of the conceptual design trade space for distributed satellite systems. By comparing architectures through comprehensive metrics based on information network theory, GINA produces more than single point designs – GINA actually helps find new cost effective design architectures. Coupled with MDO algorithms, GINA provides the system engineer with a tool to make, during the conceptual design stage of a program, intelligent architecture decisions that will directly impact lifecycle cost and performance.

Space-based GMTI radar systems have the potential to achieve a high probability of detection for small, slow-moving targets. Current single aperture systems have produced exciting results, but the future lies with separated spacecraft interferometry. Constellations of multiple aperture clusters will soon provide complete global coverage of potentially life-threatening developments around the world at lower cost and risk than current airborne systems. The design of such a system requires careful consideration of the signal processing used to combine a series of received radar signals to synthesize in the radar footprint. SPIR, provides near-ideal clutter rejection, albeit at some computational cost. With ever-increasing computational power, this should not place an undue burden on system design. One of the most significant advantages of SPIR is that performance is independent of the type of clutter.

Imaging of terrestrial targets at resolutions that are beyond the capability of a single aperture is made possible with the advent of the interferometer. In this work, an innovative trajectory design that exploits the properties conic sections while using optical delay lines to image off-nadir targets was also presented. The analysis used in this work can be extended to imaging stellar objects from within Earth's orbit. The difference in this case is to consider an inertially pointed system instead. Since it is more important to obtain high angular resolution images and not full coverage, the collector optics in this case are usually small. As such, comparison between the different designs should be dependent upon the propellant required to keep the spacecraft in formation. In addition, an algorithm to determine the optimal trajectories to re-orient a cluster of spacecraft has been developed. The problem, framed as an optimal control problem, was solved using the well known linear-quadratic controller, namely a system with linear dynamics and quadratic costs. Terminal constraints geared towards the Techsat 21 mission were also developed

A new set of linearized equations of motion have been developed for satellite formation flying. These equations of motion are similar to Hill's equations in the form and ease of use, but at the same time capture the effect of the  $J_2$  disturbance force. The development of these equations of motion brings insight to satellite cluster dynamics and provides a tool for developing trajectory optimization and control algorithms.

The selection of the precision formation flying propulsion systems for the five missions examined in this study was based on three major criteria. They include performance, cost and technical feasibility. Performance is judged by the ability to meet specified mission requirements. Cost is based on hardware manufacturing, launch and necessary research and development. While not included quantitatively, the technical feasibility of developing a propulsion technology is discussed and used to influence the recommendation of propulsion systems for implementation on the missions. It was shown that all of the propulsion systems examined have potential areas of usefulness. Additionally, it was seen that the extent of technological development of a propulsion technology can have a large impact on the financial resources necessary for its implementation on a given mission.

Distributed Satellite Sparse Apertures (DSSAs) revolutionize mission evolution from experimental demonstration to operational readiness. Experimental demonstration essentially involves check-out of the first element in the array. Once proven on orbit, confidence exists to launch additional elements on an as-needed, as-afforded basis. Technology upgrades can be incorporated in additional elements and the arrays can be grown beyond their original capabilities. DSSAs also pose new and complex challenges. In addition to currently envisioned formation flight, close proximity formation flight, electromagnetic control, and rendezvous and docking may be needed. After rendezvous and docking, precision alignment, power and propulsion cross-strapping, and control reconfiguration become essential. Inter-satellite navigation and metrology that is expandable as the array grows and autonomous operations for fault detection and recovery, fuel balancing, docking, and control reconfiguration are needed.

Use of an optimization solver electronically linked to a launch vehicle database provides tremendous versatility to the solution of the launch vehicle selection problem. This is especially important when working in the dynamic space launch market. New launch vehicles with differing capabilities and costs can be introduced, failures can ground operational launch vehicles, or quotas and export license blocks can be placed on vehicles from different countries by Congress or the State Department. The Launch Vehicle Selection Tool presented in this report can be used to quickly and effectively find a new, optimized launch vehicle selection strategy for the full deployment, replacement, or replenishment of the satellites within a constellation.

The SPHERES project has been tested in two different settings: the one-g laboratory setup and the KC-135 reduced gravity airplane micro-gravity environment. The laboratory tests served to prove the overall functionality of the SPHERES testbed. The tests demonstrated operational propulsion, communications, software, power, and inertial metrology systems. Further work is being done to improve the global metrology system. Even in its early stages, the SPHERES testbed has provided insights into the use of Formation Flight algorithms. Therefore, the testbed will continue to be used to mature the different algorithms that will enable this technology.

The successful layering of hardware and software provided a multi-agent simulation environment capable of representing essential cluster behaviors such as communication and coordination. Subsequent addition of a dynamic simulation environment and a more complex function enable more complete understanding of the factors affecting autonomous implementations of sparse aperture using spacecraft clusters.

The AIT digital signal processing is most directly analogous to astronomical radio systems. An astronomical radio-frequency cluster is a difficult concept to envision since the spacings between elements would have to be huge. Very Long Baseline Interferometry uses a combination of ground and space observations. A 'cluster' solely devoted to radio interferometry would have to be of similar size to add greater functionality. At such sizes, it would resemble a large constellation rather than a closely-knit cluster. The capacity for coordinated actions would be greatly reduced. On the other hand, localized clusters would be acceptable in a ground looking radar system. The specific processing methods are different but the distribution and autonomy issues are similar. With some adjustment in the signal processing algorithms, such a system would be very well represented by AIT operation.

GRRDE and GFLOPS have demonstrated excellent capabilities as a tool for developing space flight software and an environment for simulating distributed satellite systems. The GRRDE approach to software design has proven to be very beneficial to flight software development in our simulations, minimizing development and debugging time. The study has also demonstrated the suitability of OSE as a real-time distributed operating system and of embedded C++ as a programming language for FSW. The ongoing simulation of the TechSat21 system will provide an invaluable analysis of this mission, allowing for investigation of possible processing architectures, parameter optimization and autonomy integration.

All of these technologies are key to the success of future distributed satellite systems. From cradle to grave, distributed satellite system engineering presents a new and innovative way of implementing space assets to enable previously unobtainable performance in a highly volatile time of military demand and budget.

## References

---

- [1] Cantafio, Leopold (editor). *Space Based Radar Handbook*, Artech House, 1989.
- [2] Klemm, R. "Introduction to Space-Time Adaptive Processing", *IEEE Electronics & Communication Engineering Journal*, Volume 11, Issue 1, February 1999.
- [3] Sedwick, R.J.; Hacker, T.L.; Marais, K., *Performance Analysis for an Interferometric Space-Based GMTI Radar System*, Radar Conference, The Record of the IEEE 2000 International, May 2000, Virginia.
- [4] Marais, K., Sedwick, R. J., *Space Based GMTI Using Scanned Pattern Interferometric Radar (SPIR)*, IEEE Aerospace Conference, Proceedings of, March 2001, Montana, 0-7803-6599-2/01.
- [5] Larson, Wiley J., Wertz, James R. eds. *Space Mission Analysis and Design*. Torrance, CA: Microcosm, Inc., 1992.
- [6] Mankins, J. C. "Technology Readiness Levels: A White Paper," <http://rel.jpl.nasa.gov/Org/5053/qual/tecready.htm>, Advanced Concepts Office, Office of Space Access and Technology, NASA, April 6, 1995.
- [7] Spencer, David T. "New Millennium Program Space Technology 6 Technology Announcement," [http://nmp.jpl.nasa.gov/st6/st6\\_ta.pdf](http://nmp.jpl.nasa.gov/st6/st6_ta.pdf), California Institute of Technology, October, 10, 2000.
- [8] Sedwick, R.J., D.W. Miller and E.M.C. Kong, "Mitigation of Differential Perturbations in Clusters of Formation Flying Satellites", AAS 99-124, accepted for publication in the *Journal of Astronautical Sciences*, 2000.
- [9] Meyer, K. W., Chao, C. C., "Atmospheric Reentry Disposal for Low-Altitude Spacecraft," *Journal of Spacecraft and Rockets*, pp 670-674, Vol. 37, No. 5, September-October, 2000.
- [10] Enright, J. *Investigation of Spacecraft Cluster Autonomy Through An Acoustic Imaging Testbed*, MIT-SERC Report 8-99, 1999
- [11] Cornwell, Tim and Bridle, Alan *Deconvolution Tutorial*, National Radio Astronomy Observatory, Web reference <http://www.cv.nrao.edu/~abridle/deconvol/deconvol.html>, 1996
- [12] Marais, K., Sedwick, R. J., "Space Based GMTI Using Scanned Pattern Interferometric Radar (SPIR)", *IEEE Aerospace Conference, Proceedings of*, March 2001, Montana, 0-7803-6599-2/01.
- [13] Thomson, A. Richard; Moran, James M. and Swenson, George W. Jr., *Interferometry and Synthesis Techniques in Radio Astronomy*, Krieger Publishing Company, Malabar Florida, 1994.
- [14] *New World Vistas: Air and Space Power for the 21<sup>st</sup> Century*, USAF Scientific Advisory Board, 1995.
- [15] The official EC++ website is: <http://www.caravan.net/ec2plus/>.

---

## BIBLIOGRAPHY

### Section 2.1

Jilla, C.D., and Miller, D.W., "Assessing the Performance of a Heuristic Simulated Annealing Algorithm for the Design of Distributed Satellite Systems," *Acta Astronautica*, Vol. 48, No. 5-12, 2001.

Jilla, C.D., Miller, D.W., and Sedwick, R.J., "Application of Multidisciplinary Design Optimization Techniques to Distributed Satellite Systems," *Journal of Spacecraft and Rockets*, Vol. 37, No.4, 2000, pp. 481-490.

Miller, D.W., Curtis, A., De Weck, O., Frazzoli, E., Girerd, A., Hacker, T., Jilla, C.D., Kong, E.M., Makins, B., and Pak, S., "Architecting the Search for Terrestrial Planets and Related Origins (ASTRO)," *Proceedings of the SPIE International Symposium on Astronomical Telescopes and Instrumentation 2000*, SPIE 4013-74, Munich, Germany, March 2000.

Shaw, G.B., Miller, D.W. and Hastings, D.E., "Generalized Characteristics of Satellite Systems," *Journal of Spacecraft and Rockets*, Vol. 37, No. 6, 2000, pp. 801-811.

Shaw, G.B., Miller, D.W., and Hastings, D.E., "Development of the Quantitative Generalized Information Network Analysis (GINA) Methodology for Satellite Systems," *Journal of Spacecraft and Rockets*, Vol. 38, No. 2, 2001, pp. 257-269.

### Section 2.2

Marais, K., Sedwick, R. J., "Cluster Design for Scanned Pattern Interferometric Radar (SPIR)", AIAA Space 2001 Conference, Proceedings of, August 2001, Albuquerque, 2001-4654.

### Section 2.3

Kong, E.M.C., Miller, D.W., and Sedwick, R.J., "Optimal Trajectories and Orbit Design for Separated Spacecraft Interferometry", MIT Space Engineering Research Center Report #13-98, November 1998.

Kong, E.M.C., Miller, D.W., and Sedwick, R.J., "Exploiting Orbital Dynamics for Aperture Synthesis Using Distributed Satellite Systems: Applications to a Visible Earth Imager System", *The Journal of the Astronautical Sciences*, Vol 47, Nos 1 and 2, Jan – Jun 1999.

Kong, E. M. C., and Miller, D. W., "Minimum Energy Trajectories for Techsat 21 Earth Orbiting Clusters", AIAA Space 2001 Conference and Exposition, 28-30 August, 2001.

Kong, E. M. C., and Miller, D. W., "Optimal Spacecraft Re-Orientation for Earth Orbiting Clusters: Applications To Techsat 21", 51<sup>st</sup> International Astronautical Congress, Rio de Janeiro, Paper No. IAF-00-A.4.06, 2-6 October, 2000.

---

#### Section 2.4

S. A. Schweighart, R. J. Sedwick, "Development and Analysis of a High Fidelity Linearized  $J_2$  Model for Satellite Formation Flying", AIAA #2001-4744, AIAA Space 2001 Conference, , Albuquerque, NM., August 28-30, 2001.

S. A. Schweighart, R. J. Sedwick, "A Perturbative Analysis of Geopotential Disturbances for Satellite Cluster Formation Flying", IEEE Aerospace Conference, Big Sky Montana, 2001.

#### Section 2.7

Barrett, Anthony, "Autonomy Architectures for a Constellation of Spacecraft", International Symposium on Artificial Intelligence Robotics and Automation in Space (ISAIRAS), Noordwijk, The Netherlands, June 1999.

Desai, Jaydev P., Kumar, Vijay, Ostrowski, James P., "Control of changes in Formation for a Team of Mobile Robots," Proceeding of the IEEE International Conference on Robotics and Automation, Detroit, May 1999, pp 1556-1561.

Folta, David C., and Quinn, David, "A 3-D Method for Autonomously Controlling Multiple Spacecraft Orbits", IEEE Aerospace Conference, 21-28 March, 1998, IEEE Catalog Number 98TH8339, Vol. 1, pp 51-60.

Hartman, Kate R., Gramling, Cheryl J., Lee, Taesul, Keibel, David A., and Long, Anne C., "Relative Navigation for Spacecraft Formation Flying", AAS 98-353, American Astronautics Society/Goddard Space Flight Center 13th International Symposium on Space Flight Dynamics, Vol 2, pp 635-649, May 1998.

Robertson, Andrew, Inalhan, Gokhan, How, Jonathan P., "Spacecraft Formation Flying Control Design for the Orion Mission," AIAA Paper 99-4266.

Wang, P.K.C., Hadaegh, F. Y., and Lau, K., "Synchronized Formation Rotation and Attitude Control of Multiple Free-Flying Spacecraft", Journal of Guidance, Control, and Dynamics, Vol. 20 No. 1, pp 28-35, January-February 1999.

#### Section 2.9

Munson, J.E., and Jilla, C.D., "An Optimization Approach to the Launch Vehicle Selection Process for Satellite Constellations," *Proceedings of the 18th AIAA International Communications Satellite Systems Conference*, Oakland, CA, April 2000.

#### Section 2.11

Hacker, T.L., Sedwick, R.J., and Miller, D.W., "Performance Analysis of a Space-Based GMTI Radar System Using Separated Spacecraft Interferometry," SERC Report # 2-2000, MIT Space Systems Laboratory, Cambridge, MA, May 2000.

---

**Section 2.12**

Saenz-Otero, Alvar, Miller, David W., "The SPHERES Satellite Formation Flight Testbed: Design and Initial Control", MIT Masters of Engineering Thesis, Department of Electrical Engineering and Computer Science, September 2000.

Miller, David W., et al, "SPHERES Design Document", MIT SSL internal document , v2.0, November 1999.

Miller, David W., et al, "SPHERES Requirements Document", MIT SSL internal document, v2.0, April 1999.

Miller, David W., et al, "SPHERES Safety Requirements and Verification Data Package: Phase 0", MIT SSL internal document, Nov 1999.



## BIBLIOGRAPHY OF DSS PUBLICATIONS (REFERENCED BY CD SECTION)

BIBLIOGRAPHICAL INFORMATION	Section
Jilla, C. D. and Miller, D. W., "Satellite Design: Past, Present, and Future," <i>International Journal of Small Satellite Engineering</i> , Vol. 1, Issue 1, ISSN 1360-7014, July 1997.	2.1
Jilla, C. D. and Miller, D. W., "A Reliability Model for the Design and Optimization of Separated Spacecraft Interferometer Arrays," 11th AIAA/USU Conference on Small Satellites, SSC-97-XI-2, Sept. 1997, Logan, UT.	2.2
Enright, J., Jilla, C., and Miller, D., "Modularity and Spacecraft Cost," <i>Journal of Reducing Space Mission Cost</i> , 1:133-158, 1998.	2.3
Shaw, G., "The Generalized Information Network Analysis Methodology for Distributed Satellite Systems", Doctor of Science Thesis, MIT Department of Aeronautics and Astronautics, October 1998.	2.4
Shaw, G. B., Miller, D. W., and Hastings, D. E., "Development of the Quantitative Generalized Information Network Analysis (GINA) Methodology for Satellite Systems," <i>AIAA Journal of Spacecraft and Rockets</i> , Vol 38, #2, March-April, 2001, pgs. 257-269.	2.5
Shaw, G. B., Miller, D. W., and Hastings, D. E., "Generalized Characteristics of Satellite Systems," <i>AIAA Journal of Spacecraft and Rockets</i> , Vol. 37, #6, Nov-Dec, 2000, pgs. 801-811.	2.6
Jilla, C.D., Miller, D.W., and Sedwick, R.J., "Application of Multidisciplinary Design Optimization Techniques to Distributed Satellite Systems," <i>Journal of Spacecraft and Rockets</i> , Vol. 37, No. 4, 2000, pp. 481-490.	2.7
Jilla, C., and Miller, D. W., "Assessing the Performance of a Heuristic Simulated Annealing Algorithm for the Design of Distributed Satellite Systems," 51 <sup>st</sup> International Astronautical Congress, October 2000, Rio de Janeiro, Brazil.	2.8
Sedwick, R.J., T.L. Hacker and D.W. Miller, "Optimum Aperture Placement for a Space-Based Radar System Using Separated Spacecraft Interferometry," AIAA Guidance, Navigation, and Control Conference, August 9-11, 1999, Portland, OR.	3.1.1
Hacker, T.L. and R.J. Sedwick, "Space-Based GMTI Radar Using Separated Spacecraft Interferometry," AIAA Space Technology Conference, AIAA 99-4634, September 28-30, 1999, Albuquerque, NM.	3.1.2
Sedwick, R.J., T.L. Hacker, K. Marais, "Performance Analysis for an Interferometric Space-Based GMTI Radar System," IEEE 2000 International Radar Conference, May 7-12, 2000, Alexandria, VA.	3.1.3
Marais, K. and R.J. Sedwick, "Space Based GMTI Using Scanned Pattern Interferometric Radar," IEEE 2001 Aerospace Conference, March 2001, Big Sky, MT.	3.1.4
Marais, K. and R.J. Sedwick, "Cluster Design for Scanned Pattern Interferometric Radar," AIAA #2001-4654, AIAA Space 2001 Conference, August 28-30, Albuquerque, NM.	3.1.5

Kong, E.M., and Miller, D.W., "Optimization of Separated Spacecraft Interferometer Trajectories in the Absence of A Gravity-Well," SPIE's International Symposium on Astronomical Telescopes and Instrumentations, Paper no. 3350-13, March 1998.	3.2.1
Kong, E. M., "Optimal Trajectories and Orbit Design for Separated Spacecraft Interferometry," Master of Science Thesis, MIT Department of Aeronautics and Astronautics, 1998.	3.2.2
Sedwick, R.J., Miller, D.W., and Kong, E.M., "Mitigation of Differential Perturbations in Clusters of Formation Flying Satellites," <i>The Journal of the Astronautical Sciences</i> , Vol. 47, Nos. 3 and 4, July - December, 1999.	4.1.1
Schweighart, S.A. and R.J. Sedwick, "A Perturbative Analysis of Geopotential Disturbances for Satellite Cluster Formation Flying," IEEE 2001 Aerospace Conference, March 2001, Big Sky, MT.	4.1.2
Schweighart, S.A., "Development and Analysis of a High Fidelity Linearized J2 Model for Satellite Formation Flying," Master of Science Thesis, MIT Department of Aeronautics and Astronautics, June 2001.	4.1.3
Schweighart, S.A., R.J. Sedwick, "Development and Analysis of a High Fidelity Linearized J2 Model for Satellite Formation Flying," AIAA #2001-4744, AIAA Space 2001 Conference, August 28-30, Albuquerque, NM.	4.1.4
Mallory, G.J., Jilla, C.D., and Miller, D.W., "Optimization of Geosynchronous Satellite Constellations for Interferometric Earth Imaging," Proceedings of the 1998 AIAA/AAS Astrodynamics Specialist Conference, Paper AIAA-98-4379, August 1998.	4.2.1
Sedwick, R.J., E.M.C Kong and D.W. Miller, "Exploiting Orbital Dynamics and Micropropulsion for Aperture Synthesis Using Distributed Satellite Systems: Applications to TechSat 21," AIAA Defense and Civil Space Program Conference, AIAA-98-5289, October 28-30, 1998, Huntsville, AL.	4.2.2
Kong, E.M.C., Miller, D.W. and Sedwick, R.J., "Exploiting Orbital Dynamics for Aperture Synthesis Using Distributed Satellite Systems: Applications to a Visible Earth Imager System," <i>The Journal of the Astronautical Sciences</i> , Vol. 47, Nos. 1 and 2, January - June, 1999.	4.2.3
Kong, E.M.C., Miller, D.W., and Sedwick, R.J., "Exploiting Orbital Dynamics for Stellar Separated Spacecraft Interferometry," American Control Conference, ACC99-I014-04, June 1999.	4.2.4
Kong, E.M.C., Tollefson, M.V., Skinner, J.M., and Rosenstock, J.C., "TechSat21 Cluster Design using AI Approaches and the Cornwell Metric," AIAA Space Technology Conference and Exposition, September 1999.	4.2.5
Kong, E.M.C., Miller, D.W., and Sedwick, R.J., "Trajectory Design for A Visible Geosynchronous Earth Imager," AIAA Space Technology Conference and Exposition, September 1999.	4.2.6
Kong, E. M. C., and Miller, D. W., "Optimal Spacecraft Re-Orientation for Earth Orbiting Clusters: Applications to Techsat 21," 51 <sup>st</sup> International Astronautical Congress, IAF-00-A.4.06, October 2000, Rio de Janeiro, Brazil.	4.2.7
Reichbach, J., "Micropropulsion System Selection for Precision Formation Flying Satellites," Master of Science Thesis, MIT Department of Aeronautics and Astronautics, January 2001.	4.3.1

Saenz-Otero, A., "The SPHERES Satellite Formation Flight Testbed: Design and Initial Control," Master of Engineering Thesis, MIT Department of Electrical Engineering and Computer Science, August 2000.	4.4.1
Enright, J., Sedwick, R., and Miller, D., "High Fidelity Simulation for Spacecraft Autonomy Development," <i>ASTRO-2000 11<sup>th</sup> CASI Conference on Astronautics</i> , Nov. 6-9, 2000, Ottawa, Ontario.	4.4.2
Saenz-Otero, A., and Samidh Chakrabarti, "Implementing MiniME in the SPHERES Testbed," MIT 16.412 Intelligent Embedded System Term Project Report, December 2000.	4.4.3
Enright, J., Sedwick, R., and Miller, D., "An Evolutionary Approach to Engineering Spacecraft Flight Software," <i>IASTED Applied Informatics 2001: Software Symposium</i> , Feb. 19-22, 2001, Innsbruck, Austria.	4.4.4
Munson, J.E., and Jilla, C.D., "An Optimization Approach to the Launch Vehicle Selection Process for Satellite Constellations," Proceedings of the 18th AIAA International Communications Satellite Systems Conference, April 2000, Oakland, CA.	5.2
Andringa, J., "A Systems Study on How to Dispose of Fleets of Small Satellites," Master of Science Thesis, MIT Department of Aeronautics and Astronautics, February 2001.	5.3
Jilla, C.D. and Miller, D.W. "Separated Spacecraft Interferometry System Architecture Design and Optimization," Master of Science Thesis, MIT Department of Aeronautics and Astronautics, 1998.	6.1
Jilla, C.D., and Miller, D.W., "Separated Spacecraft Interferometry – System Architecture Design and Optimization on the Basis of a Cost Per Function Metric," Proceedings of the 3 <sup>rd</sup> International Symposium on Reducing the Cost of Spacecraft Ground Systems and Operations, Paper MP-3, March 1999.	6.2
Curtis, A., et al. "ASTRO: Architecting the Search for Terrestrial Planets and Related Origins," MIT Space Systems Laboratory, SERC #6-99, 1999.	6.3
Miller, D.W., Curtis, A., De Weck, O., Frazzoli, E., Girerd, A., Hacker, T., Jilla, C.D., Kong, E.M., Makins, B., and Pak, S., "Architecting the Search for Terrestrial Planets and Related Origins (ASTRO)," Proceedings of the SPIE International Symposium on Astronomical Telescopes and Instrumentation 2000, SPIE 4013-74, March 2000, Munich, Germany.	6.4
Hacker, T., "Performance Analysis of a Space-Based GMTI Radar System Using Separated Spacecraft Interferometry," Master of Science Thesis, MIT Department of Aeronautics and Astronautics, May 2000.	6.5
Miller, D., et. al., "SPHERES: A Testbed for Long Duration Satellite Formation Flying in Micro-Gravity Conditions," AAS/AIAA Space Flight Mechanics Meeting, AAS 00-110, January 23-26, 2000, Clearwater, FL.	7.1.1
Enright, J. "Investigation of Spacecraft Cluster Autonomy Through An Acoustic Imaging Testbed," MIT Department of Aeronautics and Astronautics, September 1999.	7.2.1

## DISTRIBUTION LIST

DTIC/OCP 8725 John J. Kingman Rd, Suite 0944 Ft Belvoir, VA 22060-6218	1 cy
AFRL/VSIL Kirtland AFB, NM 87117-5776	2 cys
AFRL/VSIH Kirtland AFB, NM 87117-5776	1 cy
MIT Space Systems Laboratory Attn: Prof. David W. Miller 77 Mass Ave. Rm 37-371 Cambridge, MA 02139	1 cy
Official Record Copy AFRL/VSSV/Mr. Ted Williams	1 cy